Modulation of plant chemistry by rhizosphere bacteria

Jeon, J.

Chapter 3

The metabolic signature of rhizobacteria-induced growth promotion in different plant species

Je-Seung Jeon, Natalia Carreno-Quintero, Ric De Vos,
Jos M. Raaijmakers and Desalegn W. Etalo

Manuscript under revision for publication

Abstract

Various rhizobacteria promote plant growth and trigger systemic resistance against leaf pathogens and phytophagous insects. To date, however, the underlying chemistry and metabolic signatures of these rhizobacteria-induced plant phenotypes are less understood. To identify core metabolic pathways that are targeted by growth-promoting rhizobacteria, we used combinations of three plant species and three rhizobacterial species and interrogated the plant shoot chemistry by untargeted metabolomics. Our results showed that a substantial part (50-64%) of the metabolites detected in host shoot tissue was differentially regulated by the rhizobacteria. Among others, the phenylpropanoid pathway was targeted by the rhizobacteria in each of the plant species. Differential regulation of the various branches of the phenylpropanoid pathways showed an association with either plant growth promotion or growth reduction. Overall, suppression of flavonoid biosynthesis was associated with growth promotion, while growth reduction showed elevated levels of flavonoids. Our study also showed that a number of pharmaceutically and nutritionally important metabolites in the plant shoot were significantly increased by rhizobacterial root treatment, providing new avenues to use rhizobacteria to tilt plant metabolism towards the biosynthesis of valuable natural plant products.

Keywords: beneficial rhizobacteria; plant metabolomics; bacteria-plant interactions; phenylpropanoids; flavonoids, metabolic alterations

Introduction

The rhizosphere, the narrow zone (± 1-2 mm) surrounding and influenced by plant roots, harbors a plethora of soil-borne microorganisms that can have deleterious or beneficial effects on plant growth and health (Raaijmakers *et al.*, 2009; Mendes *et al.*, 2013). Amongst the best-studied beneficial rhizosphere microbes are the Plant Growth-Promoting Rhizobacteria (PGPR). Their beneficial association is thought to be ancient and presumably has been shaped by co-evolutionary processes in the long-term interactions with their host plants (Lambers *et al.*, 2009). PGPR can enhance plant growth through direct and indirect mechanisms (Lugtenberg & Kamilova, 2009). The direct mechanisms involve facilitation of nutrient acquisition and modulation of phytohormones, whereas indirect effects involve reducing the inhibitory effects of biotic stress factors through parasitism, antibiosis, competition and the induction of systemic resistance (L. C. van Loon *et al.*, 1998; De Vleesschauwer & Höfte, 2009; Lugtenberg & Kamilova, 2009; Van der Ent *et al.*, 2009; Pineda *et al.*, 2010; Stringlis, I. A. *et al.*, 2018).

PGPR can also have profound effects on the physiology and metabolism of their host plants, not only by enhancing the production of known secondary metabolites but also by inducing the biosynthesis of yet-unknown compounds (van de Mortel *et al.*, 2012). The plant secondary metabolites affected by PGPR reported to date include, among others, polyphenols, flavonoids and glucosinolates but also primary metabolites such as carbohydrates and amino acids (Etalo *et al.*, 2018). So far, only a few studies have provided insights into the association between rhizobacteria-induced biochemical changes and plant growth and defense (Walker *et al.*, 2011; van de Mortel *et al.*, 2012; Weston *et al.*, 2012; Etalo *et al.*, 2018; Hu *et al.*, 2018; Stringlis, Ioannis A *et al.*, 2018).

PGPR can prime plant defense against pathogens and insect herbivores and at the same time promote plant growth. This is in contrast to the widely accepted concept of the trade-off between plant defense and plant fitness in general and plant growth in particular. Understanding the underlying growth- and defense-associated plant metabolic networks and unraveling their interactions is essential to understand and optimize rhizobacteria-mediated growth promotion and ISR. Although some reports indicated rhizobacteria-mediated changes in specific metabolites classes (Mishra *et al.*, 2006; Walker *et al.*, 2011; Chamam *et al.*, 2013), their overarching effects on the global metabolome of plants and in particular on core metabolite pathways that are co-occurring with growth promotion across plant species are not well understood. More specifically, PGPR-mediated re-routing of the plant's metabolism could give insight into the metabolic interplay between plant defense and growth. Furthermore, it is highly instrumental to understand the organization of metabolite routes, which consequently contribute to the engineering of the plant metabolism by tilting a particular pathway towards a desired target. Recently, PGPR-induced metabolic changes have attracted the interests of researchers for the development of new strategies to enhance the production of high value plant compounds (HVPC) (Etalo *et al.*, 2018).

Here, we studied the impact of three strains of different rhizobacterial genera on the phenotype and shoot metabolome of three plant species: *Arabidopsis thaliana* (model plant), *Brassica olearacea* var. italica (crop) and *Artemisia annua* (medicinal plant). Our primary interest was to identify core metabolic pathways that are targeted by rhizobacteria in different plant species and investigated their regulation under effective and ineffective rhizobacteria-plant partnerships that lead to plant growth promotion or growth reduction, respectively. A combination of *in vitro* bioassays and untargeted metabolomics was used to examine common and specific plant responses triggered by these different rhizobacterial strains. Our results show that inoculation of the plant root system with each of these rhizobacteria induced substantial changes in the shoot metabolome in a species-specific manner. Both growth-promoting and growth-reducing plant-rhizobacteria combinations revealed that the phenylpropanoid pathway is central to the plant metabolome response and that differential regulation of different branches of this pathway showed an association with positive and negative effects of the rhizobacteria on plant growth.

Materials and Methods

Plant material and growth

For *in vitro* experiment, seeds of *Arabidopsis thaliana* Columbia (Col-0) and *Artemisia annua* (kindly provided by Artemisia F1seed, Department of Biology, University of York, England) were surface sterilized as previously described (van de Mortel *et al.*, 2012). Seeds of *Brassica olearacea* var. italica, cultivar Coronado (kindly provided by Bejo Seeds, Warmenhuizen, the Netherlands) were surface sterilized for 30 min in 1% (v/v) sodium hypochlorite and 0.1 % (v/v) Tween 20 and then washed three times with ample sterile distilled water. After sterilization, seeds were pre-germinated on wet filter paper in plastic petri dishes and placed at 4 °C in the dark for 2 to 4 days. After the emergence of the radicle, seeds were sown on half-strength Murashige and Skoog (MS) medium containing 2.5% (w/v) sucrose and plant agar 12%. The plates were then transferred to a climate chamber at 21 °C /21 °C day/night; 180 µmol light $m^{-2}s^{-1}$, 16h light/8h dark cycle and 70% relative humidity. After 7 days for *A. thaliana* and *A. annua* and 3 days for *B. oleracea,* 2 µl of a washed bacterial cell suspension (OD_{600} = 1.0) was inoculated onto the root tips of the seedlings. After inoculation, plants were grown in the same growth chamber until harvest.

Bacterial strains and culture conditions

The rhizobacterial species *Paraburkholderia graminis* (*Pbg*) (Carrión *et al.*, 2018) and *Microbacterium* (MB) (Cordovez *et al.*, 2018) used in this study were originally isolated from the rhizosphere of sugar beet *Beta vulgaris*. *Pseudomonas fluorescens* (*Pf* SS101) was isolated from wheat rhizosphere (de Souza *et al.*, 2003). *Pf* SS101 was cultured in King's medium B (KB), while MB was cultured in Tryptone Soy broth (TSB) medium and *Pbg*

in Luria Bertani (LB) medium (Lennox, Carl Roth) at 25 °C for 16h. Bacterial cells were collected by centrifugation, washed three times with 10 mM $MgSO_{4,}$ and resuspended in 10 mM $MgSO_4$ to a final density of ~10^9 cells/ml (OD_{600} = 1.0).

Plant phenotyping

Fresh biomass of plant shoots was determined every two days until 11 days post inoculation (dpi) for Arabidopsis and Broccoli and 14 dpi for Artemisia. For each plant species, four independent biological replicates were used with 10 seedlings of Arabidopsis, 8 of Artemisia and 5 of Broccoli per biological replicate. Prior to root dry mass measurements, roots were carefully detached from the MS-agar and washed with sterile distilled water to remove agar. Thereafter, root dry biomass was determined (Ostonen *et al.*, 2007). Student's *t*-Test and two-way ANOVA were used to determine statistically significant ($P < 0.05$) differences between treatments.

Rhizobacteria colonization

Bacterial root colonization was determined at 11 dpi for Arabidopsis and Broccoli and at 14 dpi for Artemisia. Roots were collected in sterile glassware and their weight was determined. Root samples were vortexed for 60 s in 10 mM $MgSO_4$, sonicated for 60 s, and vortexed once more for 15 s. After serial dilution, 50 µl of the suspensions were plated onto PSA (*Pf* SS101 and *Pbg*) and TSA (MB) containing 100 µg ml^{-1} delvocid (DSM). After 3 days incubation at 25 °C, the number of colonies were determined for each of the replicates. Bacterial colonization was expressed as colony-forming units (cfu) per gram of root fresh weight.

Plant metabolite analysis

Sample collection and extraction

Shoots were harvested at 11 dpi for Arabidopsis (N=10) and Broccoli (N=5) seedlings, and at 14 dpi for Artemisia (N=8). For each plant species x rhizobacteria combination, 4 biological replicates comprising the aforementioned number of plants were used. Briefly, shoots were snap frozen in liquid nitrogen and ground to a fine powder under continuous cooling and kept at -80 °C until further use. For extraction of semipolar metabolites, 300 µL of 99.89% methanol containing 0.13% (v/v) formic acid was added to 100 mg powdered plant material in 2 ml round bottom Eppendorf tubes, and sonicated for 15 min followed by centrifugation for 15 min at 20,000 X*g*. The supernatants were transferred to a 96-well plate (AcroPrepTM, 350 µL, 0.45µm, PALL) and vacuum filtrated into a 96-deep-well autosampler plate (Waters) using a Genesis Workstation (Tecan Systems).

Metabolite analysis

An UltiMate 3000 U-HPLC system (Dionex) was used to create a 45 minutes linear gradient of 5-35% (v/v) acetonitrile in 0.1% (v/v) formic acid (FA) in water at a flow rate of 0.19 ml min^{-1}. 5 µl of each extract was injected and compounds were separated on a Luna C18 column (2.0 x 150 mm, 3µm; Phenomenex) maintained at 40 °C (De Vos *et al.*, 2007). The detection of compounds eluting from the column was performed with a Q-Exactive Plus Orbitrap FTMS mass spectrometer (Thermo Scientific). Full scan MS data were generated with electrospray in switching positive/negative ionization mode at a mass resolution of 35,000 (FWHM at m/z 200) in a range of m/z 95-1350. Subsequent MS/MS experiments for identification of selected metabolites were performed with separate positive or negative electrospray ionization at a normalized collision energy of 27 and a mass resolution of 17,500. The ionization voltage was optimized at 3.5 kV for positive mode and 2.5 kV for negative mode; capillary temperature was set at 250 °C; the auxiliary gas heater temperature was set to 220 °C; sheath gas, auxiliary gas and the sweep gas flow were optimized at 36, 10 and 1 arbitrary units, respectively. Automatic gain control was set a 3^{e6} and the injection time at 100 ms. External mass calibration with formic acid clusters was performed in both positive and negative ionization modes before each sample series.

LCMS data processing and analysis

Mass peak picking and alignment were performed using Metalign software (Lommen, 2009). Mass features in the resulting peak list were considered as a real signal if they are detected with an intensity of more than 3 times the noise value and in 3 out of the 4 biological replicates of at least one treatment. Mass features originating from the same metabolites were subsequently reconstituted based on their similar retention window and their intensity correlation across all measured samples, using MSClust software (Tikunov *et al.*, 2012). This resulted in the relative intensity of 725 putative metabolites in Arabidopsis, 868 in Artemisia and 1908 in broccoli, in which the metabolite abundance was represented by the Measured Ion Count (MIC), i.e the sum of the corrected intensity values of all mass features ions within the corresponding cluster. ANOVA and a threshold of at least a 2-fold change were applied to pinpoint compounds that were significantly different between rhizobacteria-treated and control samples. Log transformation and scaling of the data was performed in GeneMaths XT 1.6 (www.applied-maths.com). Transformed and scaled values were used for hierarchical cluster analysis using Pearson's correlation coefficient and Unweighted Pair Group Method with Arithmetic Mean (UPGMA).

Annotation of differential metabolites was performed after manually identifying the putative molecular ions within the clustered masses. In-house database was used to annotate metabolites detected in Arabidopsis and Broccoli by considering the observed accurate masses and retention times of the molecular ions. Secondly, if selected compounds were not

yet present in this experimentally obtained database, detected masses were matched with compound libraries, including Metabolomics Japan (www.metabolomics.jp), the Dictionary of Natural Products (http://dnp.chemnetbase.com), KNApSAcK (http://kanaya.naist.jp/KNApSAcK), and Metlin (http:// metlin.scripps.edu/) using a maximum mass deviation of 5 ppm. To annotate metabolites detected in Artemisia, we used the online Magma (Ridder *et al.*, 2013) in combination with the above-mentioned publicly available databases.

Statistical analysis

The relative changes in shoot biomass, root biomass in the combinations of the three plants and three rhizobacterial strains was analyzed with R Studio (Version 3.5.2). First, the normality and homogeneity of variance of the data was assessed and when the two assumptions are not met, the data was transformed using Box-Cox transformation using the package MASS. Differences were tested by two-way analysis of variance (ANOVA). A Tukey-HSD test was used to separate group mean values when the ANOVA was significant at $p < 0.05$. The ANOVA table is shown in Supplementary Material, **Table S1**. Differences between rhizobacterial treatments and non-treated control on raw phenotype parameters were compared by Student's *t*-Test.

Results

Plant growth promotion is bacteria and plant species-specific

To assess the magnitude of the changes in growth of Arabidopsis (a model plant), Artemisia (a medicinal plant) and Broccoli (a crop) upon rhizobacterial treatment (**Fig 1**), we used the percent change in fresh biomass of root and shoot relative to the non-treated, germ-free control plants. Two-way ANOVA showed that the impact of the three rhizobacteria on plant growth was highly dependent on the interacting partners (Supplementary Material, **Table S1**).

Effective partnerships

Root tip inoculation with *Pf* SS101 resulted in a significant increase in shoot biomass in both Arabidopsis and Artemisia (63.1% ± 4.7 and 38.7% ± 6.3, respectively) (**Fig 1a2**). Similarly, root tip inoculation with *Pbg* resulted in significant increases in shoot biomass of both Artemisia and Broccoli (470.4% ± 21.3 and 54.1% ± 11.9, respectively). Considering the relative increase in shoot biomass, *Pbg*-Artemisia was the most striking partnership with a biomass increase of almost 5-fold relative to the untreated control plants. Likewise, the effect of the rhizobacterial strains on root biomass was highly species-specific. *Pbg* resulted in significant increases in root biomass in both Artemisia and Broccoli (773.9% (± 28.2) and 258.8% (± 50.1), respectively) (**Fig 1b2**). To assess the temporal changes in plant growth, the time-dependent changes in plant biomass of the respective bacteria-plant combinations

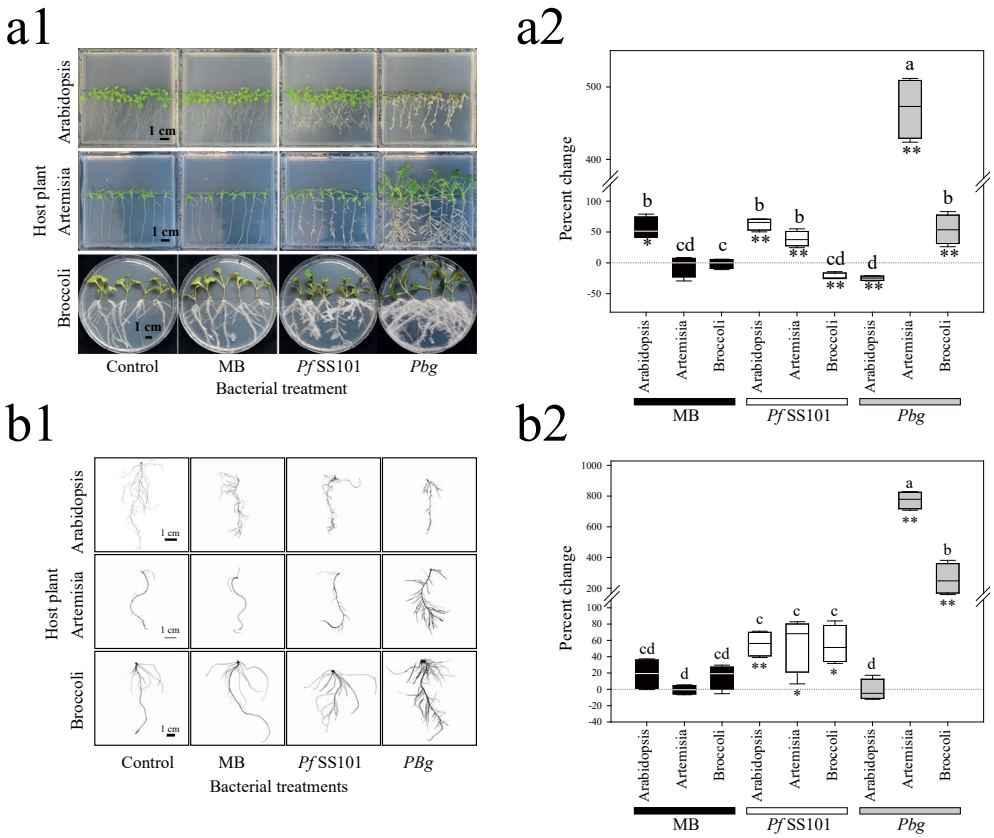

Fig 1. Phenotypic changes in response to rhizobacteria inoculation. Photographs of MS agar plates with Arabidopsis, Artemisia and Broccoli seedlings at 11/14/11 dpi, respectively (**a1**). Percent change in shoot fresh biomass (**a2**). Root morphology changes in response to rhizobacteria inoculation (**b1**). Percent change in root fresh biomass (**b2**). *Pf* SS101: *Pseudomonas fluorescens* SS101, MB: Microbacterium sp, Pbg: Paraburkholderia graminis. Asterisks denote statistical differences (two tailed Student's t test): * $P < 0.05$; ** $P < 0.01$. Means of percent changes with a different letter are significantly different based on Two way ANOVA (Tukey, $P < 0.05$).

were used as a measure (**Fig 2**). The best-performing combinations were characterized by an early and sustained growth promotion. For example, the combination *Pbg*-Artemisia showed a significant increase in shoot fresh biomass as early as 5 dpi, while growth promotion in the combination *Pf* SS101-Artemisia was only apparent after 13 dpi (**Fig 2c**). *Pbg*-Broccoli showed a significant and sustained plant growth promotion at 7 dpi compared to the control plants (**Fig 2b**). In Arabidopsis, only *Pf* SS101 induced a significant increase in shoot biomass (**Fig 2a**).

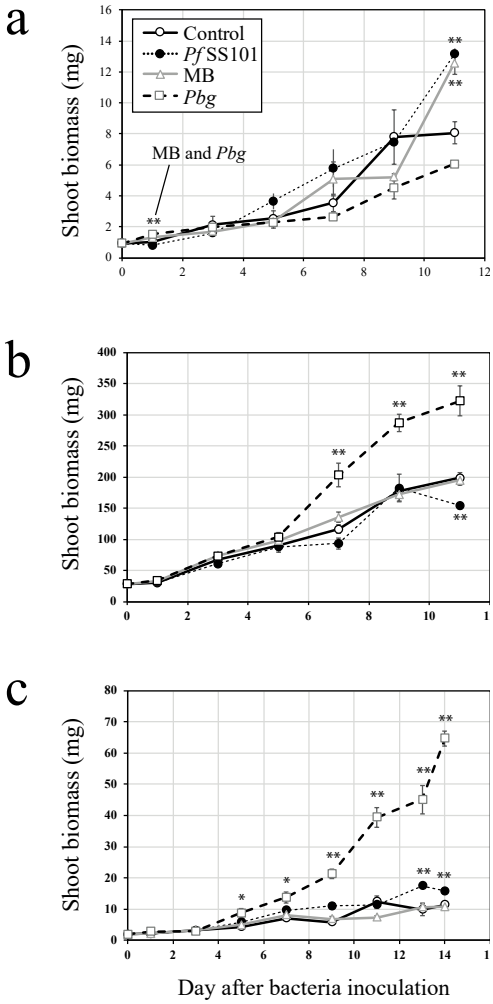

Fig 2. Temporal dynamics of growth of Arabidopsis **(a)**, Broccoli **(b)** and Artemisia **(c)** after inoculation with three distinct rhizobacterial strains. *Pf* SS101: *Pseudomonas fluorescens* SS101, MB: *Microbacterium* sp., : *Paraburkholderia graminis*. Error bars represent the standard error of the mean. Asterisks denote statistically significant differences (two tailed Student's t test): * $P < 0.05$; ** $P < 0.01$

Ineffective partnerships

Root tip inoculation of *Pf* SS101 resulted in a significant reduction (-22% ± 2.6) of the shoot biomass in Broccoli. Similarly, inoculation of Arabidopsis with *Pbg* significantly reduced the shoot biomass (-24.9% ± 1.8). Root tip inoculation of both Artemisia and Broccoli with MB had no significant impact on both shoot and root biomass (**Fig 1a2**).

Relationship between growth promotion and root colonization

In the gnotobiotic assays described here, root colonization was assessed when plants were 11 days old. Root colonization by *Pf* SS101 was considerable for Arabidopsis, Broccoli and Artemisia with populations ranging from $1.5 \pm 0.1 \times 10^5$ to $9.4 \pm 0.7 \times 10^7$ CFU·mg^{-1} root fresh weight. In contrast, MB colonization of roots varied greatly between different plant species: MB established population densities on Arabidopsis roots of $7.5 \pm 0.5 \times 10^6$ CFU·mg^{-1}, whereas on Artemisia roots MB densities were below the detection limit (2.3 CFU mg^{-1}). *Pbg* colonized roots of all three plant species at relatively high densities ranging from $8.1 \pm 0.3 \times 10^7$ to $1.0 \pm 0.1 \times 10^9$ CFU·mg^{-1} (Supplementary Material, **Table S2**). To determine correlations, if any, between the rhizosphere population densities and specific plant phenotypes (i.e. biomass), we plotted the rhizobacterial densities against various plant parameters (Supplementary Material, **Fig S2**). Colonization of the root at higher density showed a positive, negative or no association with the shoot and root biomass depending on the host-rhizobacteria combination. For example, *Pbg* showed higher population densities, compared to *Pf* SS101 and MB, on the root of Arabidopsis and Artemisia.

In Arabidopsis, high population densities of *Pbg* were associated with a significant reduction in shoot biomass while in Artemisia it resulted in substantial enhancement of the shoot biomass. In Broccoli, all three rhizobacterial strains showed a similar level of root colonization: *Pbg* showed significant increase in shoot biomass while *Pf* SS101 resulted in significant reduction in shoot biomass and MB showed no significant growth promotion. Hence, there was no clear overall correlation between root colonization and shoot biomass (Supplementary Material, **Fig S2a**). The lack of an overall association between root colonization and shoot biomass was also found for the root biomass (Supplementary Material, **Fig S2b**).

Global and specific rhizobacteria-induced changes in the plant shoot metabolome

LC-MS-based non-targeted metabolite profiling was used to investigate the global and specific effects of each of the three rhizobacterial strains on the occurrence and relative abundance of semi-polar secondary metabolites of Arabidopsis, Artemisia and Broccoli. Particular emphasis was given to investigate the metabolic alterations that differentiate effective from ineffective plant-rhizobacteria partnerships. An overview of metabolites that were significantly increased or reduced revealed that root inoculation with *Pbg* exerted the largest alteration of the shoot metabolome of Artemisia and Arabidopsis, combinations that represent the most effective and infective partnerships, respectively. Furthermore, most of the differential metabolites were unique for plants inoculated with *Pbg*, i.e they were below the detection limit in control plants. In Broccoli, the ineffective partnership with *Pf* SS101 accounted for the largest share of the 'upregulated' metabolites, whereas its effective partnership with *Pbg* accounted for the largest share of 'down-regulated' metabolites (**Fig 4a**). ANOVA with correction for multiple testing (Benjamini and Hochberg), principal component analysis (PCA) and hierarchical cluster analysis (HCA) were performed to investigate and visualize metabolite clusters that were significantly altered ($p < 0.05$, fold change > 2) in a rhizobacteria-plant specific manner (**Fig 3**). Below, we will discuss the most significant changes for each of the three plant species induced by the respective rhizobacterial strains.

Arabidopsis

Inoculation of Arabidopsis roots with each of the three rhizobacteria resulted in significant changes in the shoot metabolome. From the total of 725 metabolites that were detected in both positive and negative ionization mode, 465 (64%) metabolites were significantly different between at least two treatments. In the PCA, the first three principal components explained 89% of the total variance (**Fig 3a**). The first principal component (PC1), representing 56% of the total variance, was associated with metabolites that were highly induced (**Fig 3b** clusters **5**; 291 metabolites and **6**; 10 metabolites) or reduced in the ineffective partnership between *Pbg* and Arabidopsis (clusters **3**; 82 metabolites and **4**; 33 metabolites). *Pbg*-induced metabolites in cluster **5** primarily encompassed flavonoid glycosides including anthocyanins (cyanidin rutinoside, delphinidin rutinoside), tryptophan and its derivatives such as IAA, defense

or stress-associated metabolites such as salicylic acid, dihydroxybenzoic acid glucosides, scopolin and camalexin. The second principal component (PC2) explained 21% of the total variance and corresponded to metabolites that were increased (**Fig 3a and b**, clusters **2**; 18 metabolites and **6**; 9 metabolites) or decreased (cluster **7**; 10 metabolites) in the effective partnership of Arabidopsis with *Pf* SS101 and MB. Among the identified metabolites, the long-chain aliphatic glucosinolate glucohirsutin (8-(methylsulfinyl)octyl glucosinolate) was significantly increased in Arabidopsis shoot after inoculation with *Pf* SS101 or MB. From the same group of glucosinolates, 8-(methylthio) octyl glucosinolate was significantly increased after inoculation with *Pf* SS101 (Supplementary Material, **Table S4**). The third principal component (PC3) explained 12% of the total variation and was represented by metabolites that accumulated only after inoculation with either *Pf* SS101 or MB (**Fig 3a,** cluster **1**; 8 metabolites and cluster **9**; 7 metabolites, respectively). A fatty acyl glycoside demonstrated *Pf* SS101-specific accumulation while fumaric acid displayed MB-specific increases.

Broccoli

Similar to Arabidopsis, inoculation of Broccoli roots with each of the three rhizobacterial strains resulted in substantial alteration of the shoot metabolome. From the total of 1908 metabolites that were detected in either positive or negative ionization modes, 933 (49%) were significantly different between at least two treatments. For this set of metabolites, HCA revealed 8 distinct metabolite clusters of the host metabolome. Similar to Arabidopsis, PCA showed that the metabolome of Broccoli seedlings inoculated with different rhizobacteria is clearly different from the control and from each other. The first three PCs explained 84% of the total variance (**Fig 3c**). PC1, representing 47% of the total variance, was associated with metabolites that discriminate both the control and MB samples from the *Pbg* and *Pf* SS101 samples. These metabolites were either highly increased or highly decreased in plants inoculated by *Pbg* or *Pf* SS101 (**Fig 3d** decreased cluster **3** and induced clusters **6** and **7**) that represents effective and ineffective partnership with the host, respectively. The anticancer indole glucosinolate glucobrassicin also showed a significant increase in plants inoculated with *Pbg* and *Pf* SS101. PC2 explained 22% of the total variance and corresponded to metabolites that were either specifically altered in the *Pbg* or *Pf* SS101 treatments (**Fig 3d** induced (clusters **8** (*Pf* SS101) and **9** (*Pbg*)) or reduced by *Pbg* inoculation (cluster **4**)). Metabolites that were specifically induced in the ineffective partnership between *Pf* SS101 and the host were dominated by flavonoids such as kaempferol, quercetin glycosides and glucosinolates including glucoibervirin, neoglucobrassicin and 4-methoxyglucobrassicin. Furthermore, a number of hydroxycinnamates with or without conjugation with quinic acid, including chlorogenic acid (caffeoyl-quinic acid), coumaroyl quinic acid, sinapic acid and ferulic acid, were predominant in this metabolite cluster (cluster **7**). PC3 explained 15% of the total variation and corresponded to MB-induced metabolites represented in cluster **1** and induced metabolites by all three rhizobacteria in cluster **2**. Hexose 1-phosphate in cluster **1** showed a MB-specific increase. Meanwhile, some of the putatively annotated metabolites in

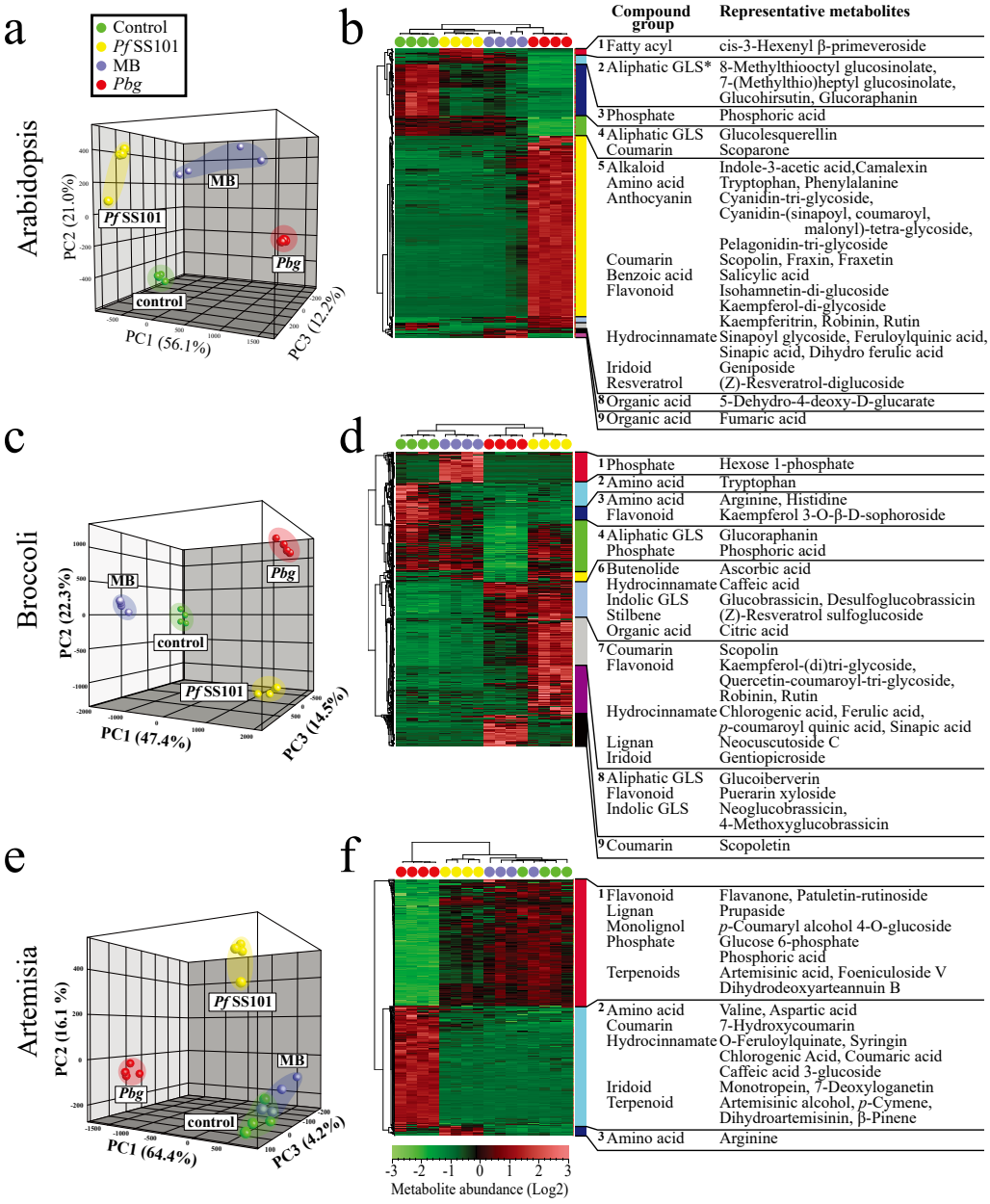

Fig 3. Rhizobacteria-mediated changes in the shoot metabolome. Shown are PCA and HCA results based on differentially regulated semi-polar metabolites in the shoot of Arabidopsis (**a** and **b**), Broccoli (**c** and **d**) and Artemisia (**e** and **f**) after root inoculation with three different rhizobacteria (*Pf* SS101: *Pseudomonas fluorescens* SS101, MB: *Microbacterium* sp. and *Pbg*: *Paraburkholderia graminis*). * GLS=glucosinolate, ** d=derivative. In the HCA, metabolite clusters are indicated by different colors and when none of the metabolites in a given cluster was annotated, the cluster number is omitted (clusters 6 and 7 in (b) and cluster 5 in (d)).

cluster **2** including tryptophan, a precursor of indole glucosinolates was reduced by all three rhizobacterial treatments.

Artemisia

From the total of 868 metabolites that were detected in the Artemisia shoot samples, 451 (52%) metabolites were significantly different between at least two rhizobacteria treatments. Unlike that of Arabidopsis and Broccoli, HCA revealed only few distinct metabolite clusters in Artemisia in response to the rhizobacteria (**Fig 3f**). In the PCA, the first two PCs explained 80% of the total variance (**Fig 3e**). The first principal component explained more than 64% of the total variance and corresponds to metabolites that were either reduced or enhanced during the most effective partnership of the host with *Pbg* (**Fig 3f** cluster **1 (**reduced metabolites) and cluster **2** (induced metabolites)). Flavanones, flavonol glycosides, coumarins, benzoic acid derivatives, acylated polyamine, catechin, fatty acyl glycosides of mono- and disaccharides, dipeptide and terpene glycosides showed significant reductions upon *Pbg* inoculation. Various other metabolites belonging to the compound classes hydroxycinnamoyl quinic acids and derivatives, organic acids, mono and diterpenoids, and iridoids showed a significant increase after root inoculation with *Pbg*. Treatment of Artemisia with *Pbg* resulted in significant reduction in artemisinic acid while the relative levels of both dihydroartemisinin and artemisinic alcohol significantly increased. PC2 explained 16% of the total variance and corresponded to induced metabolites (cluster **3**) in response to *Pf* SS101 inoculation. Putative metabolite identification revealed that the amino acid arginine, fatty acyl glycoside blumenol glycoside and phenylpropanoid glycoside derivatives were induced in a *Pf* SS101-specific manner.

Comparative analysis of rhizobacteria-induced plant shoot metabolome changes

The metabolome changes induced by the different rhizobacteria in the shoots of Arabidopsis and Broccoli were subjected to a comparative analysis as both plant species belong to the Brassicaceae family. Although total glucosinolate levels in shoots of both Brassica species were commonly upregulated by *Pf* SS101, glucosinolate subcategories were altered in a rhizobacteria-specific manner. For instance in Arabidopsis, the effective partnership with *Pf* SS101 enhanced the relative levels of aliphatic long-chain glucosinolates such as glucohirsutin and 8-methylthiooctyl glucosinolate, whereas the infective partnership between *Pf* SS101 and Broccoli led to an increase in the levels of indolic glucosinolates (i.e. glucobrassicin, desulfoglucobrassicin, 4-methoxyglucobrassicin and neoglucobrassicin) and short-chain aliphatic glucosinolates such as glucoibervirin. In contrast to the effective *Pf* SS101-Arabidopsis partnership, the ineffective *Pbg*-Arabidopsis partnership caused a drastic reduction of all detected aliphatic glucosinolates, (i.e. glucohirsutin (8-methylsulfinyloctyl glucosinolate), glucolesquerellin (6-methylthiohexyl glucosinolate), 7-methylthioheptyl glucosinolate and 8-methylthiooctyl glucosinolate. In Broccoli, both its ineffective partnership

with *Pf* SS101 and its effective partnership with *Pbg* caused significant increases of the indolic glucosinolate glucobrassicin. Meanwhile, the effective MB-Arabidopsis partnership led to upregulation of glucohirsutin while this rhizobacterial strain barely influenced the level of glucosinolates in Broccoli (Supplementary Material, **Table S5**). Flavonoids, on the other hand, were shown to respond in a more rhizobacteria-specific manner. In Arabidopsis, flavonoids were predominantly enhanced by both *Pbg* and MB treatments while in Broccoli

a

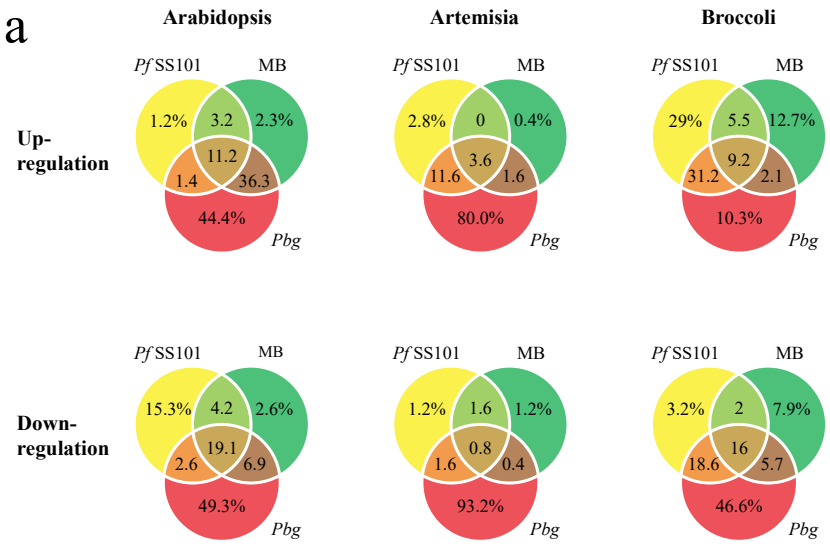

b

Plant	Rhizobacteria	Increased metabolites			Decreased metabolites		
		Total	Ionization		Total	Ionization	
			+	-		+	-
Arabidopsis	***Pf* SS101**	59	38	21	75	45	33
	MB	184	105	79	62	36	26
	Pbg	324	183	141	147	85	62
Artemisia	***Pf* SS101**	45	24	21	13	8	5
	MB	14	11	3	10	8	2
	Pbg	243	134	109	245	130	115
Broccoli	***Pf* SS101**	585	303	282	201	120	81
	MB	230	143	87	160	85	75
	Pbg	411	203	208	439	235	204

Fig 4. Rhizobacteria-mediated global changes in the shoot metabolome of the three different plant species. The Venn diagrams display the distribution of unique and shared differentially regulated metabolites in shoots of Arabidopsis, Artemisia and Broccoli **(a)**. Presented values are the sum of differentially regulated metabolites detected in either positive or negative ionization modes. Total number of metabolites increased and decreased in abundance based in either positive or negative ionization mode are presented in **(b)**. Further details are provided in Supplementary Table 2. *Pf* SS101: *Pseudomonas fluorescens* SS101, MB: *Microbacterium* sp., *Pbg*: *Paraburkholderia graminis*.

Pf SS101 elevated the level of many flavonoids (Supplementary Material, **Table S5**). Combination of Arabidopsis with *Pbg* and MB, and Broccoli with *Pf* SS101 represent ineffective partnerships. In conclusion, comparative metabolomics of the two Brassicaceae plant species suggests that regulation of particular biosynthetic pathways is rhizobacteria specific and host species dependent. Alteration to a particular branch of phenylpropanoid pathway showed co-occurrence with growth promotion (effective partnership) or growth reduction (ineffective partnership) in cross-species plant-rhizobacteria combination. Most interestingly, metabolite identification led to a list of natural products that are presumed to exert health promoting or pharmaceutically important effects during both effective and ineffective partnership between plants and rhizobacteria. The list of various metabolites that are presumed to have specific functions are summarized in Supplementary **Table S7**.

Discussion

Over the past decades, several studies indicated that beneficial rhizobacteria promote plant growth, induce systemic resistance against pathogens and phytophagous insects and can alter plant secondary metabolism (Van Peer *et al.*, 1991; Walker *et al.*, 2011; van de Mortel *et al.*, 2012; Etalo *et al.*, 2018; Hu *et al.*, 2018; Stringlis, Ioannis A *et al.*, 2018). Our results confirm and extend the importance of rhizobacteria in plant growth promotion (Barriuso *et al.*, 2008; van de Mortel *et al.*, 2012; Castanheira *et al.*, 2016; Cordovez *et al.*, 2018) and provide a unique insight into the global metabolome changes and specific plant metabolic signatures of effective and ineffective partnerships between rhizobacteria and their host plant. Effectiveness refers in this study to an interaction that resulted in growth promotion. Of the three tested rhizobacterial genera, none of the strains showed growth-promoting effects for all three different plant species indicating specificity in rhizobacteria-plant interactions. For example, *Pbg* established an effective partnership with Artemisia and Broccoli whereas interaction with Arabidopsis was deleterious given the significant reduction in biomass and the accumulation of stress-related dark-purple anthocyanins in the leaves (**Fig 1a1**). Even when there is effective partnership between rhizobacteria and the host, the extent of growth promotion can significantly differ as shown by the partnership of *Pbg* with Artemisia and Broccoli. The temporal analyses of the rhizobacteria-host interactions also demonstrated that establishment of effective partnership was characterized by early and sustained induction of growth promotion as was typically the case for the *Pbg* interaction with Artemisia and Broccoli (**Fig 2**). The differential growth response of the three plant species to *Pbg* inoculation exemplifies the need for finding the right partnership between rhizobacteria and host plant. The establishment of high population densities of PGPR on root is claimed to be associated with plant growth promotion. This may explain the lack of phenotypic responses of Artemisia to MB inoculation. However, our results also indicated that high rhizosphere population densities of the introduced strains can be associated with either growth promotion or growth reduction as was seen for the combination of *Pbg* with Artemisia (growth promotion) and *Pbg*

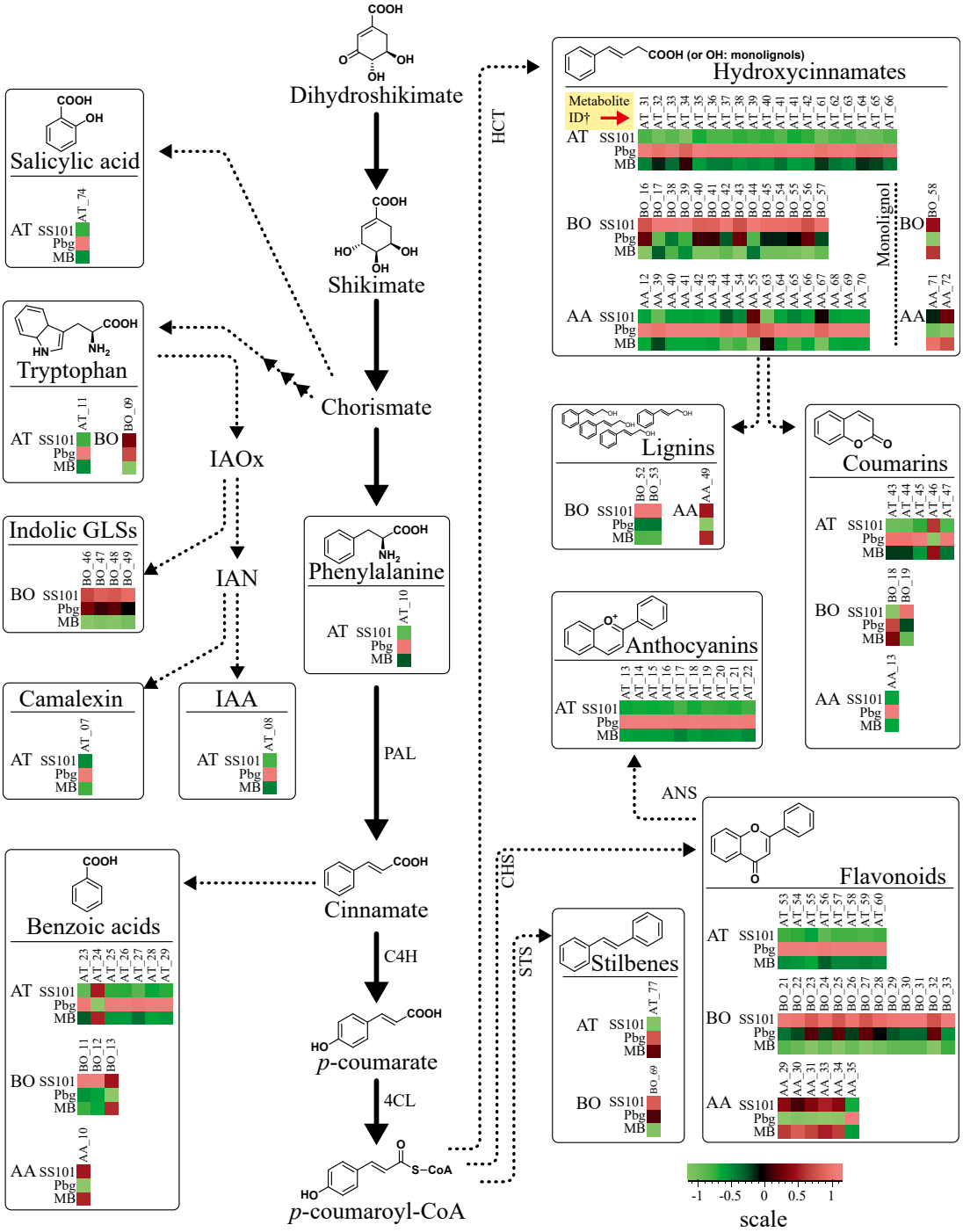
Dihydroshikimate
Shikimate
Chorismate
Salicylic acid
Tryptophan
IAOx
IAN
Indolic GLSs
Camalexin
IAA
Phenylalanine
PAL
Cinnamate
C4H
p-coumarate
4CL
p-coumaroyl-CoA
Benzoic acids
HCT
CHS
STS
ANS
Hydroxycinnamates
COOH (or OH: monolignols)
Metabolite ID†
Monolignol
Lignins
Coumarins
Anthocyanins
Flavonoids
Stilbenes
AT SS101 Pbg MB
BO SS101 Pbg MB
AA SS101 Pbg MB
-1 -0.5 0 0.5 1
scale

Fig 5.

with Arabidopsis (growth reduction) (Supplementary Material, **Fig S2a2** and **a1**, respectively).

Generally, rhizobacteria-mediated alteration of the plant metabolome can arise from effective or ineffective partnerships. The ineffective partnership between *Pbg* and Arabidopsis is characterized by the depletion of long- and short-chain aliphatic glucosinolates and massive accumulation of metabolites from the phenylpropanoid pathway including anthocyanin and other flavonoid glycosides (**Fig 3b**, Supplementary Material, **Table S4 and Fig 5**). The accumulation of stress/defense-related metabolites such as anthocyanin and other flavonoid glycosides, camalexin, β-d-glucopyranosyl indole-3-carboxylic acid and salicylic acid (**Fig 5**) suggest that *Pbg* is perceived by Arabidopsis as a biotic stressor (Hagemeier *et al.*, 2001; Oh *et al.*, 2014; Ali *et al.*, 2018). Similarly, the ineffective partnership between Broccoli and *Pf* SS101 resulted in a significant accumulation of flavonoids (**Fig 3d**, Supplementary Material, **Table S5**). Furthermore, there was a significant increase in the level of glucobrassicin and its derivatives such as neoglucobrassicin, desulfoglucobrassicin, and 4-methoxyglucobrassicin. Interestingly, 4-methoxyglucobrassicin was reported to be a signal molecule involved in plant defense against bacteria and fungi (Bednarek *et al.*, 2009; Clay *et al.*, 2009). This suggests that Broccoli perceived *Pf* SS101 as a foe or that *Pf* SS101 induced resistance against fungal/bacterial infections. In conclusion, the above two examples suggest an association between ineffective partnerships and accumulation of flavonoids in the host shoot tissues.

The metabolome profile of Arabidopsis inoculated with *Pbg* (an ineffective partnership) appears similar to that of the hydroxycinnamoyl transferase (HCT)-deficient Arabidopsis reported by (Besseau *et al.*, 2007). HTC and chalcone synthase (CHS) are key regulators of the phenylpropanoid pathway and influence the channeling of the key precursor *P*-coumaroyl CoA either to flavonoids or to monolignols and sinapoylmalate (**Fig 5**). Similar to the ineffective partnerships of *Pbg*-Arabidopsis or *Pf* SS101-Broccoli, HTC-mutants displayed high accumulation of flavonoids (Besseau *et al.*, 2007). Accumulation of flavonoid glycosides in Arabidopsis may affect auxin transport (Besseau *et al.*, 2007), distribution and turnover (Kuhn *et al.*, 2016), thereby affecting plant growth. Besseau *et al.* (2007) further showed that suppression of flavonoid production via CHS silencing, restored auxin transport and normal development of HCT-deficient plants. Another interesting *Pbg*-

◀◀◀ **Fig 5.** Rhizobacteria-mediated alteration of the phenylpropanoid pathway in three different plant species (*Arabidopsis thaliana* (AT), *Brassica oleracea* (BO) and *Artemisia annua* (AA)). The metabolites corresponding to the different branches of the phenylpropanoid pathway are indicated by the metabolite ID corresponding to each species and their level of accumulation is indicated by the scaled fold change corresponding to the green and red boxes for each of the metabolites. Fold change of metabolite abundance was calculated by dividing the average abundance of a metabolite in rhizobacteria treated plants to untreated control plants. For detailed information on the identity of the individual metabolites, consult the supplementary excel tables S4-S6. IAOx (indole-3-acetaldoxime), IAN (indole-3-acetonitrile), PAL (Phenylalanine ammonia-lyase), C4H (Cinnamate 4-hydroxylase), 4CL (4-coumarate-CoA ligase), CHS (Chalcone synthase), HCT (hydroxycinnamoyl-CoA shikimate/quinate hydroxycinnamoyl transferase) and STS (stilbene synthase).

induced chemotype in Arabidopsis is the accumulation of metabolites derived from the indole pathways such as IAA and camalexin. Indole-3-acetaldoxime (IAOx) plays important roles in plant development and defense response as a branching point for biosynthesis of indole glucosinolate, IAA and camalexin (Bak *et al.*, 2001). When compared to control plants, *Pbg*-treated Arabidopsis showed no significant change in the level of indole glucosinolates. However, both IAA and camalexin showed marked increases suggesting that *Pbg* inoculation leads to channeling of IAOx towards IAA and camalexin biosynthesis. Interestingly, the ineffective partnership between *Pf* SS101 and Broccoli was characterized by the accumulation of indolic glucosinolates while IAA and camalexin were not detected in the samples. Collectively, these results suggest that different rhizobacteria can influence the channeling of precursors towards specific branches of metabolic pathways involved in growth, development and/or stress tolerance in plant species-rhizobacteria specific manner. Of all rhizobacteria-plant combinations, the *Pbg*-Artemisia combination can be considered as the most effective partnership in terms of growth promotion. When compared to the control plants or plants treated with the other two rhizobacteria, the effective partnership between *Pbg* and Artemisia was hallmarked by a substantial alteration of the host metabolome (**Fig 3f** and **Fig 5**). This 'rewiring' of the Artemisia metabolome primarily involved accumulation of hydroxycinnamates and suppression of other phenolic compounds such as flavonoids and benzoic acid derivatives (**Fig 5**). *p*-Coumaroyl CoA is the central metabolite and branch-point in phenylpropanoid biosynthesis in plants. The channeling of this important precursor towards various branches of the phenylpropanoid pathway is mainly influenced by the enzymes hydroxycinnamoyl CoA:shikimate/quinatehydroxycinnamoyltransferase (HCT) and chalcone synthase (CHS) (**Fig 5**). Our results showed that one of the distinctive metabolic signatures between effective and ineffective partnerships is the differential regulation of the flavonoid pathway that is ubiquitously present in plant species. Under effective partnership, it is either suppressed or showed slight change in accumulation. Whereas, under ineffective partnership it showed high accumulation in the plant shoot (**Fig 5**). Considering our results and other reports on the negative role of flavonoids on auxin transport, auxin distribution and turnover (Jacobs & Rubery, 1988; Murphy *et al.*, 2000; Brown *et al.*, 2001; Besseau *et al.*, 2007; Kuhn *et al.*, 2011; Buer *et al.*, 2013; Kuhn *et al.*, 2016), suppression or tight regulation of flavonoids by rhizobacteria could be employed as a potential strategy to promote plant growth.

Our result clearly indicated that different rhizobacteria alter the host metabolome either in effective or ineffective partnerships. Both kinds of partnership can be employed to boost nutritionally and/or pharmaceutically important high value natural plant compounds (HVPC). For example, flavonoid glycosides induced in the ineffective partnership between *Pbg* and Arabidopsis are considered as vital phytochemicals in diets and are of great general interest due to their diverse bioactivities. Similarly, glucosinolates in Brassica species, hydroxycinnamic acid derivatives and dihydroartemisinin in Artemisia are potentially health-beneficial metabolites. In effective partnerships, the increase in these compounds is

even more pronounced when we consider the relative increase in the host biomass due to rhizobacteria inoculation. A typical example for this is the *Pbg*-Artemisia combination that resulted in five-fold increase in host biomass and up to three-fold increase per unit fresh tissue biomass in both artemisinic alcohol and dihydroartemisinin. The application of rhizobacteria to plant roots to boost economically or pharmaceutically interesting metabolites may be considered as a simple and generic approach. Moreover, breeding towards plant traits that promote the recruitment of effective rhizobacteria that induce health-promoting compounds could be considered as an alternative strategy. Understanding the underlying molecular mechanisms and traits by which beneficial rhizobacteria alter the host chemistry will be needed to optimize this microbe-mediated plant engineering strategy. This approach, referred to as "microbe Gene Positioning System (mGPS)" (Etalo et al., 2018), can be integrated with other approaches such as synthetic biology, gene-editing technologies and even with conventional breeding strategies to enhance HVPC production in crops and medicinal plants. Hence, efforts to engineer pharmaceutically and nutritionally important plant products should consider both the plant and its microbiome members as part of the puzzle.

Acknowledgements

Artemisia F1seed and Broccoli seeds were kindly provided by Department of Biology, University of York, York, UK and Bejo seed company (Trambaan1, 1749 CZ Warmenhuizen, The Netherlands), respectively. We are grateful to Bert Schipper and Henriëtte Vaneekelen for their help with LC-MS analysis and pre-processing of metabolomics data.

Supplementary materials

Table S1. Analysis of variance ANOVA (type II) of shoot and root biomass changes in three plants species inoculated with phylogenetically distinct rhizobacterial genera.

Sample	Factor	Sum Sq	Df	F value		Pr(>F)	
Shoot fresh biomass relative change	Plant species	2598.8	2	127.17		1.81E-14	***
	Bacterial species	2048.2	2	100.23		3.20E-13	***
	Plant species : Bacterial species	7500.8	4	183.53	<	2.2E -16	***
	Residuals	275.9	27				
Root fresh biomass relative change	Plant species	481.95	2	43.507		3.59E-09	***
	Bacterial species	1061.18	2	95.795		5.48E-13	***
	Plant species : Bacterial specie	1322.42	4	59.689		5.14E-13	***
	Residuals	149.55	27				
Root dry weight relative change	Plant species	894.3	2	30.101		1.338E-07	***
	Bacterial species	6860.2	2	230.893	<	2.2E-16	***
	Plant species : Bacterial species	4183.9	4	70.408		6.925E-14	***
	Residuals	401.1	27				

Significance codes: *** 0, ** 0.001, * 0.01.

Table S2. Population density of three rhizobacterial genera colonizing root of Arabidopsis (11 dpi), Artemisia (14 dpi) and Broccoli (11 dpi). *Pf* SS101: *Pseudomonas fluorescens* SS101, MB: *Microbacterium* sp., *Pbg*: *Paraburkholderia graminis*.

Plant species	*Pf* SS101	MB	*Pbg*
Arabidopsis thaliana	$9.9 \pm 0.5 \times 10^5$	$7.5 \pm 0.5 \times 10^6$	$1.2 \pm 0.1 \times 10^8$ CFU/mg*
Artemisia annua	$1.5 \pm 0.1 \times 10^5$	n.d.	$1.0 \pm 0.1 \times 10^9$ CFU/mg
Brassica oleracea	$9.4 \pm 0.7 \times 10^7$	$4.6 \pm 0.7 \times 10^7$	$8.1 \pm 0.3 \times 10^7$ CFU/mg

CFU: Colony forming unit
n.d.: not detected
*Values represent the average of 3 replicates ± SE

Table S3. Number of differentially regulated plant secondary metabolites in the shoots of Arabidopsis, Artemisia, and Broccoli after treatments of the roots with three rhizobacteria generas. *Pf* SS101: *Pseudomonas fluorescens* SS101, MB: *Microbacterium* sp., *Pbg*: *Paraburkholderia graminis*

Plant	Bacteria	Number of metabolites					
		Increased metabolites			Increased metabolites		
		Total	Ionization mode		Total	Ionization mode	
			+	-		+	-
Arabidopsis	*Pf* SS101 total	59	38	21	78	45	33
	MB_total	184	105	79	62	36	26
	Pbg total	324	183	141	147	85	62
	Pf SS101 only	4	2	2	29	17	12
	MB_only	8	5	3	5	4	1
	Pbg only	154	86	68	93	57	36
	Common in *Pf* SS101 and MB	50	32	18	44	26	18
	Common in *Pf* SS101 and *Pbg*	44	29	15	41	22	19
	Common in MB and *Pbg*	165	93	72	49	26	23
	Common in *Pf* SS101, MB, and *Pbg*	39	25	14	36	20	16
Artemisia	*Pf* SS101 total	45	24	21	13	8	5
	MB total	14	11	3	10	8	2
	Pbg total	243	134	109	245	130	115
	Pf SS101 only	7	4	3	3	2	1
	MB only	1	1	0	3	3	0
	Pbg only	201	111	90	238	128	110
	Common in *Pf* SS101 and MB	9	7	2	6	5	1
	Common in *Pf* SS101 and *Pbg*	38	20	18	6	2	4
	Common in MB and *Pbg*	13	10	3	3	1	2
	Common in *Pf* SS101, MB, and *Pbg*	9	7	2	2	1	1
Broccoli	*Pf* SS101 total	585	303	282	201	120	81
	MB total	230	143	87	160	85	75
	Pbg total	411	203	208	439	235	204
	Pf SS101 only	227	122	105	16	12	4
	MB only	99	66	33	40	12	28
	Pbg only	80	41	39	235	114	121
	Common in *Pf* SS101 and MB	115	70	45	91	56	35
	Common in *Pf* SS101 and *Pbg*	315	155	160	175	104	71
	Common in MB and *Pbg*	88	51	37	110	69	41
	Common in *Pf* SS101, MB, and *Pbg*	72	44	28	81	52	29

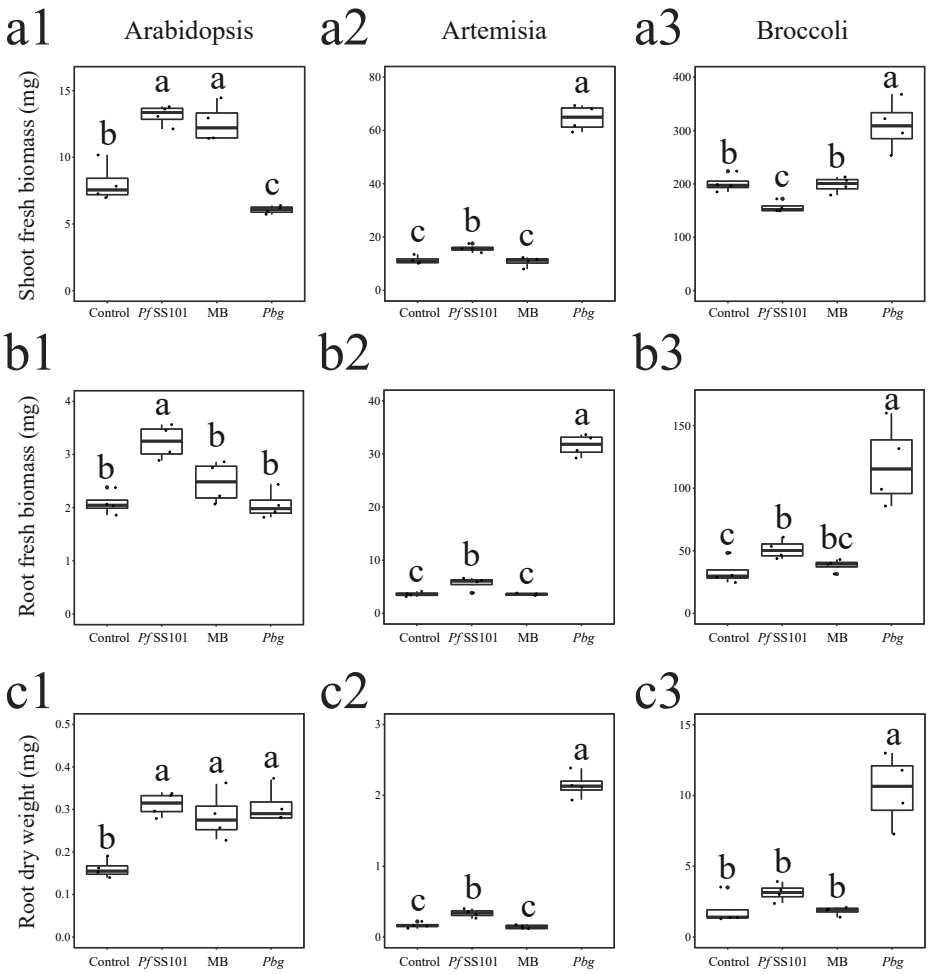

Fig S1. Rhizobacteria-mediated phenotypic changes in three plant species. Change in shoot fresh biomass **(a)**, root fresh biomass **(b)**, and root dry weight **(c)** at 11 dpi for Arabidopsis **(1)** and Broccoli **(3)** and 14 dpi for Artemisia **(2).** *Pf* SS101: *Pseudomonas fluorescens* SS101, MB: *Microbacterium* sp., *Pbg*: *Paraburkholderia graminis.* Box plots represent the average of 4 replicates. Means of percent changes with a different letter are significantly different from each other according to One-way ANOVA (Tukey, $P<0.05$).

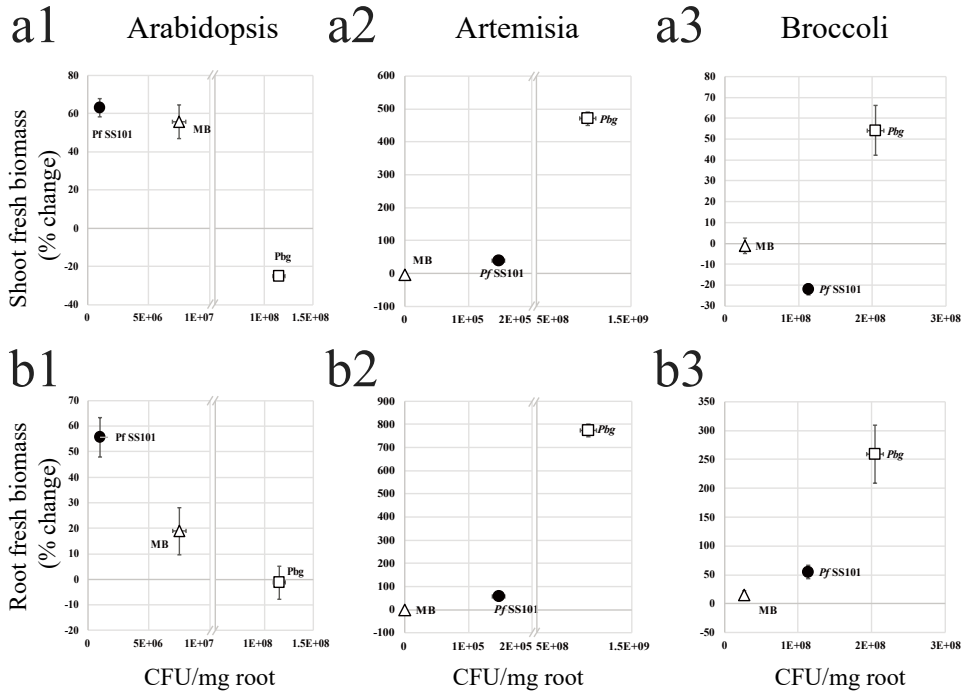

Fig S2. Correlation between rhizobacteria root colonization and host phenotypes. Correlation rhizobacterial population density (CFU/mg root) and percent changes of shoot fresh biomass **(a)** and root fresh biomass **(b)** of Arabidopsis; 11dpi **(1)**, Artemisia; 14dpi **(2)**, and Broccoli; 11dpi **(3)**. *Pf* SS101: *Pseudomonas fluorescens* SS101, MB: *Microbacterium* sp., *Pbg*: *Paraburkholderia graminis.*

Table S4. Annotation of Arabidopsis metabolites that showed significant change in their abundance after inoculation with rhizobacteria. *Pf* SS101: *Pseudomonas fluorescens* SS101, MB: *Microbacterium* sp., *Pbg*: *Paraburkholderia graminis*. Fold changes of each metabolites were calculated against non-treated control. Clustering numbers are associated with metabolite ID in **Fig 3.**

Cluster Number	Metabolite ID	RT (m)	m/z	Mass(D)	Compound	Formula	Δ ppm to DB	Classification	data base	Fold change		
										MB	*Pbg*	*Pf* SS101
1	AT_51	23.33	[M-H]-	393.176544	cis-3-Hexenyl b-primeveroside	C17H30O10	-0.2	Fatty acyl lycoside	HMDB	3.3	1.3	15.0
2	AT_02	50.35	[M-H]-	476.108398	8-Methylthiooctyl glucosinolate (8MTO)	C16H31O9S3N1	-0.9	Aliphatic GLS	KEGG	-1.0	-11.5	2.1
2	AT_01	41.47	[M-H]-	462.092896	7-(Methylthio)heptyl glucosinolate	C15H29O9S3N1	-0.5	Aliphatic GLS	KEGG	-1.0	-16.4	1.7
2	AT_03	20.40	[M-H]-	492.103516	Glucohirsutin	C16H31O10S3N1	-0.4	Aliphatic GLS	KEGG	3.1	-5.7	4.5
2	AT_05	2.25	[M-H]-	436.040771	Glucoraphanin	C12H23NO10S3	-0.8	Aliphatic GLS	KEGG	1.4	-25.1	1.2
3	AT_24	7.07	[M-H]-	138.055923	Gabaculine	C7H9NO2	-0.7	Benzoic acid	KEGG	-1.9	-54.5	-2.3
3	AT_72	2.49	[M+H]+	98.984619	Phosphoric acid	H3PO4	4.5	non-metal phosphate	KEGG	-2.2	-79.8	-1.5
3	AT_06	39.73	[M-H]-	416.105316	Heptylglycosinolate	C14H27O9S2N1	-1.9	Aliphatic GLS	Metlin	-3.2	-13.1	-2.9
4	AT_46	38.73	[M+H]+	207.065094	Scoparone	C11H10O4	-0.4	Coumarin	KEGG	-1.0	-23.6	1.4
4	AT_04	32.48	[M-H]-	448.077271	Glucolesquerellin	C14H27O9S3N1	-0.6	Aliphatic GLS	KEGG	-1.4	-14.5	-1.1
4	AT_76	2.98	[M+H]+	308.091278	Glutathione	C10H17N3O6S	0.7	Peptide	KEGG	-1.5	-25.6	-1.2
5	AT_07	42.55	[M+H]+	201.047867	Camalexin	C11H8N2S	2.2	Alkaloid	PubChem	12.8	64.2	20.5
5	AT_08	43.99	[M+H]+	176.070618	Indole-3-acetic acid (IAA)	C10H9NO2	0.2	Alkaloid	KEGG	14.4	39.9	8.4
5	AT_09	2.17	[M+H]+	132.101974	Leucine	C6H13NO2	0.7	Amino acid	KEGG	2.7	4.0	1.6
5	AT_10	3.57	[M+H]+	166.086349	Phenylalanine	C9H11NO2	0.4	Amino acid	KEGG	2.0	3.2	1.4
5	AT_11	6.92	[M+H]+	205.097031	Tryptophan	C11H12N2O2	-0.7	Amino acid	KEGG	1.8	6.0	1.1
5	AT_12	28.40	[M+H]+	741.222412	Anthocyanin			Anthocyanin	UV	1.2	3.3	1.3
5	AT_13	19.52	[M+H]+	757.217773	Cyanidin 3-rutinoside 5-glucoside	C33H41O20+	-0.9	Anthocyanin	KEGG	2.2	45.3	1.4
5	AT_14	27.72	[M+H]+	741.222839	Anthocyanine unidentified			Anthocyanin	UV	1.4	5.1	1.2
5	AT_15	23.22	[M+H]+	741.222961	Anthocyanine unidentified			Anthocyanin	UV	1.4	5.8	1.2
5	AT_16	27.03	[M+H]+	741.223083	Anthocyanine unidentified			Anthocyanin	UV	1.5	6.4	1.2
5	AT_18	24.81	[M+H]+	1343.349731	Cyanidin 3-O-[2-O-(2-O-(sinapoyl)-bata-D-xylopyranosyl) 6-O-(4-O-(beta-D-glucopyranosyl)-p-coumaroyl-bata-D-glucopyranoside] 5-O-[6-O-(malonyl) bata-D-glucopyranoside] I	C61H67O34	-4.1	Anthocyanin	KNApSAck +UV	87.5	1605.5	1.1
5	AT_17	26.86	[M+H]+	1344.353638	Cyanidin 3-O-[2-O-(2-O-(sinapoyl)-bata-D-xylopyranosyl) 6-O-(4-O-(beta-D-glucopyranosyl)-p-coumaroyl-bata-D-glucopyranoside] 5-O-[6-O-(malonyl) bata-D-glucopyranoside] II	C61H67O34	-4.1	Anthocyanin	KNApSAck +UV	3.6	15.2	1.0
5	AT_19	21.16	[M+H]+	741.222717	Pelargonidin 3-(2glu glucosylrutinoside)	C33H41O19	-2.0	Anthocyanin	HMDB	2.6	10.4	1.5
5	AT_20	21.78	[M+H]+	595.165222	Cyanidin 3-O-rutinoside I	C27H31O15+	-0.7	Anthocyanin	KEGG	3.9	25.9	1.6
5	AT_21	25.94	[M+H]+	595.165283	Cyanidin 3-O-rutinoside II	C27H31O15+	-0.6	Anthocyanin	KEGG	1.9	16.1	1.0
5	AT_22	23.03	[M+H]+	611.160217	Delphinidin 3-O-rutinoside	C27H31O16+	-0.5	Anthocyanin	KEGG	2.0	18.9	-1.0
5	AT_23	12.34	[M-H]-	299.077118	4-Hydroxybenzoate-O-glucoside	C13H16O8	-0.4	Benzoic acid	KEGG	1.6	7.4	-1.1
5	AT_25_2	29.40	[M-H]-	333.145416	3'-N'-Acetylfusarochromanone I	C17H22N2O5	-0.5	Benzoic acid	HMDB	2.6	16.1	1.3

Table S4. (Continued)

Cluster Number	Metabolite ID	RT (m)	m/z	Mass(D)	Compound	Formula	Δ ppm to DB	Classification	data base	Fold change		
										MB	*Pbg*	*Pf* SS101
5	AT_25	29.39	[M+H]+	335.160034	3'-N'-Acetylfusarochromanone I	C17H22N2O5	-0.3	Benzoic acid	HMDB	2.5	16.3	1.2
5	AT_26	32.68	[M+H]+	335.160065	3'-N'-Acetylfusarochromanone II	C17H22N2O5	-0.2	Benzoic acid	HMDB	2.5	18.5	1.2
5	AT_26_2	32.68	[M-H]-	333.145386	3'-N'-Acetylfusarochromanone II	C17H22N2O5	-0.6	Benzoic acid	HMDB	2.6	18.1	1.3
5	AT_27	16.45	[M-H]-	431.118896	Apiosylglucosyl 4-hydroxybenzoate	C18H24O12	-1.4	Benzoic acid	HMDB	3.1	17.2	-1.6
5	AT_28	14.66	[M-H]-	343.066803	Theogallin	C14H16O10	-0.6	Benzoic acid	KEGG	1.5	12.6	1.4
5	AT_29	11.52	[M-H]-	285.061493	Uralenneoside	C12H14O8	-0.3	Benzoic acid	HMDB	1.8	7.0	1.3
5	AT_31	12.67	[M+H]+	163.075394	Methyl cinnamate	C10H10O2	0.1	Hydroxycinnamate	KEGG	7.2	27.5	2.1
5	AT_32	36.98	[M-H]-	591.171753	1,2-Bis-O-sinapoyl-beta-D-glucoside	C28H32O14	-0.3	Hydroxycinnamate	KEGG	1.6	6.2	-2.2
5	AT_33_2	16.61	[M-H]-	385.113647	1-O-Sinapoyl beta-D-glucoside	C17H22O10	-1.0	Hydroxycinnamate	KEGG	3.0	17.8	-1.1
5	AT_33	16.60	[M+H]+	387.128021	1-O-Sinapoyl beta-D-glucoside	C17H22O10	-1.4	Hydroxycinnamate	KEGG	2.6	13.1	-1.3
5	AT_34	18.18	[M-H]-	385.1138	4-O-beta-D-Glucosyl-sinapate	C17H22O10	-0.6	Hydroxycinnamate	KEGG	1.4	3.2	-1.3
5	AT_63	11.94	[M-H]-	371.097992	Dihydroferulic acid 4-O-glucuronide	C16H20O10	-1.0	Hydroxycinnamate	HMDB	5.4	24.9	1.1
5	AT_35	37.62	[M-H]-	591.171692	Di-O-sinapoyl-beta-D-glucoside I	C28H32O14	-0.4	Hydroxycinnamate	KEGG	2.9	26.9	1.4
5	AT_36	34.73	[M-H]-	591.171753	Di-O-sinapoyl-beta-D-glucoside II	C28H32O14	-0.3	Hydroxycinnamate	KEGG	1.7	13.7	-1.5
5	AT_37	36.19	[M-H]-	591.171753	Di-O-sinapoyl-beta-D-glucoside III	C28H32O14	-0.3	Hydroxycinnamate	KEGG	1.7	12.3	-1.1
5	AT_38	33.65	[M-H]-	591.171814	Di-O-sinapoyl-beta-D-glucoside iV	C28H32O14	-0.2	Hydroxycinnamate	KEGG	2.2	13.2	1.1
5	AT_39	38.15	[M-H]-	591.17157	Di-O-sinapoyl-beta-D-glucoside V	C28H32O14	-0.6	Hydroxycinnamate	KEGG	5.0	36.3	-1.1
5	AT_66	8.41	[M+H]+	307.176392	Feruloylagmatine I	C15H22N4O3	-0.3	Hydroxycinnamate	KEGG	5.5	17.9	1.8
5	AT_66_2	8.33	[M+H]+	307.176392	Feruloylagmatine II	C15H22N4O3	-0.3	Hydroxycinnamate	KEGG	2.7	28.9	2.6
5	AT_64	36.97	[M+H]+	369.117798	O-Feruloylquinic acid	C17H20O9	-0.5	Hydroxycinnamate	KEGG	1.5	6.7	-2.4
5	AT_40_2	10.89	[M-H]-	275.151337	p-Coumaroylagmatine I	C14H20N4O2	0.0	Hydroxycinnamate	KEGG	12.2	64.0	5.2
5	AT_40	10.89	[M+H]+	277.165802	p-Coumaroylagmatine I	C14H20N4O2	-0.3	Hydroxycinnamate	KEGG	3.9	16.9	2.4
5	AT_41_2	11.34	[M-H]-	275.151337	p-Coumaroylagmatine II	C14H20N4O2	0.0	Hydroxycinnamate	KEGG	12.2	43.8	3.2
5	AT_43	10.18	[M+H]+	191.033707	Ayapin	C10H6O4	-0.9	Coumarin	KEGG	5.2	10.7	1.4
5	AT_44	10.19	[M-H]-	207.02977	Fraxetin	C10H8O5	-0.7	Coumarin	KEGG	5.3	11.4	1.4
5	AT_45	21.50	[M-H]-	369.082428	Fraxin	C16H18O10	-0.8	Coumarin	KEGG	2.1	8.4	1.4
5	AT_47	14.88	[M+H]+	355.102295	Scopolin	C16H18O9	-0.2	Coumarin	KEGG	8.6	24.8	3.3
5	AT_49	2.35	[M+H]+	244.092712	gamma-Glutamyl-beta-cyanoalanine	C9H13N3O5	-0.3	Dipeptide	KEGG	2.9	20.5	-1.1
5	AT_50	49.03	[M-H]-	545.26001	Canavalioside	C26H42O12	-0.6	Diterpene glycoside	HMDB	2.0	43.4	-1.1
5	AT_52	22.30	[M+H]+	381.175415	Prenyl arabinosyl-(1->6)-glucoside	C16H28O10	-0.3	Fatty acyl glycoside	HMDB	2.6	12.9	-1.4
5	AT_53	25.56	[M+H]+	595.1651	Kaempferol 3-galactoside-7-rhamnoside	C27H30O15	-2.0	Flavonoid	KNApSAck	2.7	9.7	1.6
5	AT_54	21.79	[M-H]-	639.156311	flavonoid di glycoside	C28H32O17	-0.6	Flavonoid	HMDB	4.0	29.4	1.5
5	AT_55	33.88	[M-H]-	609.18219	Hesperidin	C28H34O15	-0.5	Flavonoid	KEGG	-1.2	23.0	-1.1
5	AT_56	28.70	[M-H]-	623.161194	Isorhamnetin 3-neohesperidoside	C28H32O16	-0.9	Flavonoid	HMDB	2.3	3.9	1.5
5	AT_57	26.33	[M-H]-	623.161438	Isorhamnetin 3-O-[b-L-rhamnofuranosyl-(1->6)-D-glucopyranoside]	C28H32O16	-0.5	Flavonoid	HMDB	4.1	19.0	1.1

Table S4. (Continued)

Cluster Number	Metabolite ID	RT (m)	m/z	Mass(D)	Compound	Formula	Δ ppm to DB	Classification	data base	Fold change		
										MB	*Pbg*	*Pf* SS101
5	AT_58	28.68	[M+H]+	579.169983	Kaempferitrin	C27H30O14	-1.5	Flavonoid	KEGG	2.3	6.2	1.5
5	AT_53_2	25.55	[M-H]-	593.151062	Kaempferol 7-rhamnoside-4'-glucoside	C27H30O15	-0.3	Flavonoid	KEGG	2.3	4.4	1.6
5	AT_59	21.17	[M-H]-	739.20874	Robinin	C33H40O19	-0.5	Flavonoid	KEGG	2.9	8.2	1.5
5	AT_60	23.02	[M-H]-	609.145447	Rutin	C27H30O16	-1.1	Flavonoid	KEGG	2.2	21.2	-1.0
5	AT_61	3.40	[M+H]+	226.070786	4-Amino-4-deoxychorismate	C10H11NO5	-0.8	Benzoic acid	KEGG	1.3	4.9	-1.2
5	AT_41	11.35	[M+H]+	277.165771	p-Coumaroylagmatine II	C14H20N4O2	-0.4	Coumaric acids	KEGG	6.4	18.3	2.4
5	AT_65	18.17	[M+H]+	225.075516	Sinapic acid	C11H12O5	-1.2	Hydroxycinnamate	KEGG	1.5	6.0	-1.3
5	AT_62	14.89	[M-H]-	399.092651	Sinapinic acid-O-glucuronide isomer	C17H20O11	-1.6	Hydroxycinnamate	HMDB	9.0	27.3	3.2
5	AT_41_2	42.25	[M-H]-	237.076706	Trimethoxycinnamic acid I	C12H14O5	-0.6	Coumaric acids	HMDB	2.7	53.8	1.0
5	AT_41	42.22	[M+H]+	239.091248	Trimethoxycinnamic acid I	C12H14O5	-0.6	Coumaric acids	HMDB	6.7	100.3	1.4
5	AT_42	27.24	[M+H]+	239.091248	Trimethoxycinnamic acid II	C12H14O5	-0.6	Coumaric acids	HMDB	2.0	7.8	1.3
5	AT_67	18.70	[M-H]-	403.124268	Gardenoside	C17H24O11	-0.9	Iridoid	KEGG	2.3	16.6	1.3
5	AT_68	10.03	[M-H]-	549.182373	Genipin 1-beta-gentiobioside	C23H34O15	-0.3	Iridoid	KEGG	6.2	18.0	1.9
5	AT_69	12.66	[M-H]-	387.129913	Geniposide	C17H24O10	0.7	Iridoid	KEGG	8.0	30.9	2.1
5	AT_70	40.41	[M-H]-	541.192505	Deoxyloganin tetraacetate	C25H34O13	-0.2	iridoids	KEGG	-1.1	3.7	-1.9
5	AT_71	17.79	[M+H]+	124.075829	p-Anisidine	C7H9NO	1.2	Methoxyaniline	KEGG	1.3	19.7	-1.3
5	AT_74	30.98	[M-H]-	137.024216	Salicylic acid	C7H6O3	-1.5	Benzoic acid	KEGG	6.2	40.7	1.4
5	AT_75	44.69	[M-H]-	319.176056	525178	C15H28O7	-2.1	Pentaethylene glycol, monoallyl ether	PubChem	19.6	44.2	1.8
5	AT_77	20.45	[M-H]-	551.176575	(Z)-Resveratrol 3,4'-diglucoside	C26H32O13	-0.8	Resveratrol	HMDB	1.8	2.9	-1.0
8	AT_48	2.99	[M-H]-	191.019669	5-Dehydro-4-deoxy-D-glucarate	C6H8O7	-0.3	Dicarboxylic acid	KEGG	3.5	3.0	1.6
9	AT_73	3.22	[M-H]-	115.003578	Fumaric acid	C4H4O4	-1.1	Organic acid	HMDB	4.7	1.6	1.8

Table S5. Annotation of Broccoli metabolites that showed significant change in their abundance after inoculation with rhizobacteria. *Pf* SS101: *Pseudomonas fluorescens* SS101, MB: *Microbacterium* sp., *Pbg*: *Paraburkholderia graminis*. Fold changes of each metabolites were calculated against non-treated control. Clustering numbers are associated with metabolite ID in **Fig 3.**

Cluster Number	Metabolite ID	RT (m)	m/z	Mass(D)	Compound	Formula	Δ ppm to DB	Classification	data base	Fold change		
										MB	*Pbg*	*Pf* SS101
1	BO_36	2.2	[M+H]+	261.037109	Hexose 1-phosphate	C6H13O9P	0.5	Hexose phosphate	KEGG	11.4	-2.2	-1.1
2	BO_09	6.54	[M+H]+	205.097321	Tryptophan	C11H12N2O2	0.7	amino acid	KEGG	-3.0	-2.1	-2.3
2	BO_71	43.18	[M+H]+	631.276428	Brassica napus non-fluorescent chlorophyll catabolite 3	C34H38N4O8	0.3	Tetrapyrrole	HMDB	-3.0	-3.6	-4.4
2	BO_62	2.15	[M-H]-	351.10257	Benzylpenicilloic acid	C16H20N2O5S	1.6	Penicilloic acid	KEGG	-2.2	-3.9	-3.6
2	BO_05	3.20	[M-H]-	152.986389	3-Sulfolactaldehyde	C3H6O5S	0.4	Alkanesulfonic acid	KEGG	-2.8	-10.3	-8.2
3	BO_59	2.16	[M-H]-	175.047012	Allantoic acid	C4H8N4O4	-1.8	n-Carbamoyl-alpha amino acid	KEGG	-1.7	-4.9	-4.7
3	BO_34	2.98	[M-H]-	188.056656	N-Acetyl-L-glutamic acid	C7H11NO5	-2.2	Glutamic acid	KEGG	-1.7	-3.7	-3.9
3	BO_24_2	23.99	[M-H]-	609.146423	Kaempferol 3-O-beta-D-sophoroside or (C05625), (C17563), (C19796)	C27H30O16	0.5	Flavonoid	KEGG	-1.5	-8.0	-3.3
3	BO_06	1.62	[M+H]+	175.119202	Arginine	C6H14N4O2	1.3	Amino acid	KEGG	-1.2	-2.3	-2.3
3	BO_08	1.84	[M-H]-	154.062424	Histidine	C6H9N3O2	-2.9	Amino acid	KEGG, Metlin	-1.2	-2.0	-2.1
4	BO_58	33.49	[M-H]-	385.150909	Methylsyringin	C18H26O9	-0.4	Monolignol	Metlin	-1.3	-2.3	-1.4
4	BO_61	26.98	[M-H]-	593.209412	Zizybeoside II	C25H38O16	1.2	Oligosaccharide	KEGG	-1.5	-3.2	-1.2
4	BO_02	17.16	[M-H]-	380.156464	cis-Zeatin-O-glucoside	C16H23N5O6	-2.8	6-alkylaminopurines	KEGG	-1.1	-3.0	1.0
4	BO_73	12.29	[M-H]-	222.077393	Acetyl-L-tyrosine	C11H13NO4	-2.1	Tyrosine	Metlin	-1.2	-3.1	-1.2
4	BO_04	15.40	[M-H]-	436.041565	Glucoraphanin	C12H23NO10S3	1.0	Aliphatic glucosinolate	KEGG	-1.1	-2.1	1.1
4	BO_51	21.12	[M-H]-	172.098099	N-Acetylleucine	C8H15NO3	-2.7	Leucine	Metlin	1.0	-2.8	1.1
4	BO_17	19.70	[M-H]-	536.17804	4-Demethylsimmondsin 2'-(E)-ferulate	C25H31NO12	1.3	Coumaric acid	HMDB	-1.1	-2.1	1.1
4	BO_13	18.01	[M-H]-	329.088043	1-O-Vanilloyl-beta-D-glucose	C14H18O9	0.7	Benzoic acid	KEGG	-1.2	-4.6	-1.4
4	BO_60	2.53	[M+H]+	98.984688	Phosphoric acid	H3PO4	-1.5	non-metal phosphate	KEGG	-1.1	-3.0	-1.1
6	BO_72	3.00	[M-H]-	191.019897	Citric acid	C6H8O7	-2.4	Tricarboxylic acid	KEGG, Metlin	2.7	3.9	2.9
6	BO_69	34.13	[M-H]-	469.081787	(Z)-Resveratrol 3-(3''-sulfoglucoside) or (HMDB37073), (HMDB37076)	C20H22O11S	1.7	Stilbene	HMDB	1.2	2.3	2.8
6	BO_15	4.33	[M-H]-	173.009323	Dehydroascorbic acid	C6H6O6	-3.1	Bbutenolide	KEGG	1.5	2.7	3.4
6	BO_56	37.93	[M+H]+	369.118317	O-Feruloylquinic acid	C17H20O9	0.9	Hydrocinnamate	KEGG	1.1	1.9	2.2
6	BO_48	21.69	[M-H]-	447.054474	Glucobrassicin	C16H20O9S2N2	1.7	Indolic glucosinonate	KEGG	1.5	4.0	5.1
6	BO_16	17.91	[M-H]-	385.11441	1-O-Sinapoyl beta-D-glucoside	C17H22O10	1.0	Coumaric acid	KEGG	1.3	3.0	3.7
6	BO_46	21.72	[M+H]+	369.11145	Desulfoglucobrassicin	C16H20N2O6S	-0.1	Indolic glucosinolate	KEGG	1.5	3.4	3.9
6	BO_14	2.24	[M+H]+	177.039734	Ascorbic acid	C6H8O6	2.0	Butenolide	KEGG	2.0	3.7	4.5
6	BO_43	19.89	[M+H]+	195.065308	Ferulic acid or (C12204), (C10477)	C10H10O4	0.7	Hydroxycinnamate	KEGG	1.1	1.9	2.2
6	BO_40	11.40	[M+H]+	181.049728	Caffeic acid	C9H8O4	0.8	Hydroxycinnamate	KEGG	1.4	2.5	3.2
6	BO_41	11.42	[M-H]-	341.088074	Caffeic acid 3-glucoside or (C10433)	C15H18O9	0.7	Hydroxycinnamate	KEGG	1.3	2.3	2.9

Table S5. (Continued)

Cluster Number	Metabolite ID	RT (m)	m/z	Mass(D)	Compound	Formula	Δ ppm to DB	Classification	data base	Fold change		
										MB	*Pbg*	*Pf* SS101
6	BO_01	5.76	[M+H]+	298.096924	Methylthioadenosine	C11H15N5O3S	0.2	5'-deoxy-5'-thionucleoside	KEGG	1.4	2.2	2.1
7	BO_67	33.14	[M-H]-	577.156799	Glucofrangulin A	C27H30O14	0.8	Quinone	KEGG	-2.7	1.5	3.2
7	BO_50	24.09	[M+H]+	306.097595	Ascorbigen	C15H15NO6	1.2	Isosorbide	HMDB	2.2	6.4	7.1
7	BO_65	38.88	[M+H]+	339.107605	Hydrojuglone glucoside	C16H18O8	0.5	Phenolic glycoside	HMDB	2.4	4.5	8.8
7	BO_31	38.85	[M-H]-	561.162048	Flavonol 3-O-beta-D-glucosyl-(1->2)-beta-D-glucoside	C27H30O13	1.3	Flavonoid	KEGG	2.2	4.6	10.3
7	BO_42	18.74	[M+H]+	195.065338	Ferulic acid	C10H10O4	0.8	Hydroxycinnamate	KEGG	1.3	1.9	3.2
7	BO_68	18.74	[M-H]-	355.103821	Gentiopicroside	C16H20O9	1.1	Iridoid	KEGG	1.4	2.0	3.5
7	BO_07	2.04	[M-H]-	132.03035	Aspartic acid	C4H7NO4	-2.8	amino acid	KEGG	1.7	2.6	3.5
7	BO_70	2.09	[M-H]-	195.050842	D-Gluconic acid	C6H12O7	-0.9	Sugar acid	KEGG	1.3	1.8	3.2
7	BO_27	17.99	[M+H]+	935.245972	Quercetin 3-[p-coumaroyl-(->6)-glucosyl-(1->2)-glucosyl-(1->2)-glucoside] or (HMDB0029268)	C42H46O24	0.8	Flavonoid	HMDB	-1.1	1.2	2.1
7	BO_27_2	17.98	[M-H]-	933.231323	Quercetin 3-[p-coumaroyl-(->6)-glucosyl-(1->2)-glucosyl-(1->2)-glucoside]	C42H46O24	0.7	Flavonoid	HMDB	-1.1	1.2	2.3
7	BO_23	20.77	[M-H]-	947.247437	Kaempferol 3-(2-feruloylsophoroside) 7-glucoside	C43H48O24	1.2	Flavonoid	HMDB	-1.0	1.2	2.4
7	BO_25	20.78	[M+H]+	949.261597	Kaempferol 3-sophoroside 7-(2-feruloylglucoside) or (HMDB0040801), (HMDB29269)	C43H48O24	0.8	Flavonoid	HMDB	-1.1	1.3	2.3
7	BO_32	14.56	[M+H]+	773.213074	Kaempferol 3-sophorotrioside	C33H40O21	-0.5	Flavonoid	KEGG	-1.1	1.3	2.3
7	BO_53	37.39	[M-H]-	693.204773	Neocuscutoside C	C32H38O17	0.7	Lignan glycoside	Metlin	1.4	2.4	5.9
7	BO_38	40.02	[M-H]-	929.27356	2-Feruloyl-1,2'-disinapoylgentiobiose	C44H50O22	1.6	Hydroxycinnamate	HMDB	1.1	1.4	2.6
7	BO_64	26.64	[M-H]-	415.125183	2-Hydroxybenzaldehyde O-[xylosyl-(1->6)-glucoside]	C18H24O11	1.4	Phenolic glycosides	HMDB	1.7	2.1	5.7
7	BO_52	36.17	[M-H]-	693.204773	Sesaminol glucosyl-(1->2)-glucoside	C32H38O17	1.7	Lignan	HMDB	1.4	2.0	4.2
7	BO_29	20.33	[M-H]-	609.146667	Rutin	C27H30O16	0.9	Flavonoid	KEGG	1.2	1.9	3.4
7	BO_57	14.87	[M+H]+	339.107605	p-Coumaroyl quinic acid or (C10432), (C10441)	C16H18O8	0.4	Hydroxycinnamate	KEGG	1.3	2.3	3.9
7	BO_57_2	14.89	[M-H]-	337.093689	p-Coumaroyl quinic acid or (C10441), (C10432)	C16H18O8	0.4	Hydroxycinnamate	KEGG	1.3	2.3	4.2
7	BO_22	35.44	[M-H]-	723.21521	Flavonol 3-O-beta-D-glucosyl-(1->2)-beta-D-glucosyl-(1->2)-beta-D-glucoside	C33H40O18	1.4	Flavonoid	KEGG	1.5	2.6	4.3
7	BO_21	33.33	[M-H]-	577.15686	Daidzein 4',7-diglucoside	C27H30O14	1.0	Flavonoid	HMDB	1.5	2.4	5.2
7	BO_19	17.22	[M+H]+	355.102661	Scopolin or (C00852), (C08996)	C16H18O9	0.8	Coumarin	KEGG	1.2	1.9	3.1
7	BO_54	12.99	[M-H]-	371.098541	Dihydroferulic acid 4-O-glucuronide	C16H20O10	0.5	Flavonoid	HMDB	1.5	2.9	4.7
7	BO_55	10.15	[M+H]+	355.102448	Chlorogenic acid	C16H18O9	0.2	Flavonoid	KEGG	1.3	2.6	3.9
7	BO_24	20.34	[M+H]+	611.160583	Kaempferol 3-O-beta-D-sophoroside or (C05625), (C17563)	C27H30O16	-0.2	Flavonoid	KEGG	1.3	2.3	3.7
7	BO_30	28.87	[M-H]-	665.173584	sudachiin B or (HMDB0039088)	C30H34O17	1.9	Flavonoid	HMDB	1.4	2.4	5.0
7	BO_26	30.48	[M-H]-	739.210815	Mauritianin	C33H40O19	2.3	Flavonoid	HMDB	1.2	2.1	3.4

Table S5. (Continued)

Cluster Number	Metabolite ID	RT (m)	m/z	Mass(D)	Compound	Formula	Δ ppm to DB	Classification	data base	Fold change		
										MB	*Pbg*	*Pf* SS101
7	BO_45	16.68	[M+H]+	225.075836	Sinapic acid	C11H12O5	0.3	Hydroxycinnamate	KEGG	1.1	1.5	2.0
7	BO_55_2	16.11	[M+H]+	355.102692	Chlorogenic acid or (C01527), (C08996)	C16H18O9	0.9	Hydroxycinnamate	HMDB	1.7	2.9	4.5
7	BO_10	17.79	[M-H]-	278.067352	N-[4'-hydroxy-(E)-cinnamoyl]-L-aspartic acid	C13H13NO6	1.2	Aspartic acid	HMDB	1.3	2.2	3.3
7	BO_28	30.14	[M-H]-	739.210693	Robinin	C33H40O19	2.1	Flavonoid	KEGG	1.4	3.4	5.4
8	BO_49	34.54	[M-H]-	477.064697	neoglucobrassicin	C17H22O10S2N2	0.8	Indolic glucosinonate	KEGG	-1.1	1.1	3.5
8	BO_12	4.46	[M-H]-	315.072632	Ginnalin B	C13H16O9	-0.7	Benzoic acid	Metlin	1.3	1.4	7.2
8	BO_11	13.50	[M-H]-	299.077423	4-(beta-D-Glucosyloxy)benzoate	C13H16O8	0.7	Benzoic acid	KEGG	1.3	6.0	40.0
8	BO_47	27.80	[M-H]-	477.064667	4-Methoxyglucobrassicin	C17H22N2O10S2	0.7	Indolic glucosinonate	KEGG	-1.0	1.0	2.3
8	BO_33	33.93	[M-H]-	547.146606	Puerarin xyloside	C26H28O13	1.6	Flavonoids	KEGG	1.9	3.3	12.8
8	BO_20	34.36	[M+H]+	191.14299	beta-Damascenone	C13H18O	-0.3	Enone	HMDB	1.1	1.4	2.6
8	BO_03	12.11	[M-H]-	406.031067	Glucoiberverin	C11H21NO9S3	1.3	Aliphatic glucosinolate	KEGG	1.3	-1.1	2.3
8	BO_37	2.18	[M-H]-	289.033173	Sedoheptulose phosphate or (C19882)	C7H15O10P	0.5	Hexose phosphate	KEGG	1.3	-1.1	4.1
8	BO_39	16.21	[M-H]-	325.093597	4-O-beta-D-Glucosyl-4-hydroxycinnamate or (C16827)	C15H18O8	0.1	Hydroxycinnamate	KEGG	1.6	1.4	2.9
8	BO_44	16.22	[M+H]+	165.054794	p-Coumaric acid or (C00166), (C12621), (C01772)	C9H8O3	1.3	Hydroxycinnamate	KEGG	1.7	1.5	2.3
9	BO_66	2.25	[M-H]-	110.985336	Hydroxymethylphosphonate	CH5O4P	-3.5	Phosphonic acid	KEGG	1.7	3.7	3.0
9	BO_35	2.18	[M-H]-	209.066757	Coriose or (C21043), (C02076)	C7H14O7	-2.9	Glycoside	KEGG	1.8	2.9	2.2
9	BO_63	2.19	[M-H]-	306.076965	Glutathione	C10H17N3O6S	-0.7	Peptide	Metlin	1.8	2.5	1.6
9	BO_18	15.82	[M+H]+	193.049622	Scopoletin, Isoscopoletin, 4-Methyldaphnetin, 5,7-dihydroxy-4-methylcoumarin (Coumarins)	C10H8O4	0.2	Coumarin	KEGG	1.5	3.9	-8.9

Table S6. Annotation of Artemisia metabolites that showed significant change in their abundance after inoculation with rhizobacteria. *Pf* SS101: *Pseudomonas fluorescens* SS101, MB: *Microbacterium* sp., *Pbg*: *Paraburkholderia graminis*. Fold changes of each metabolites were calculated against non-treated control. Clustering numbers are associated with metabolite ID in **Fig 3.**

Cluster Number	Metabolite ID	RT (m)	m/z	Mass(D)	Compound	Formula	Δ ppm to DB	Classification	data base	Fold change		
										MB	*Pbg*	*Pf* SS101
1	AA_53	21.01	[M+H]+	209.153366	Carvyl propionate	C13H20O2	-1.1	Terpenoid	magma	1.0	-15.0	-1.7
1	AA_33	21.87	[M+H]+	565.155151	Neoschaftoside	C26H28O14	-0.1	Flavonoid	Knapsack	-1.2	-2.2	-1.2
1	AA_80	49.98	[M+H]+	235.169189	(+)-12-Hydroxy-alpha-cyperone	C15H22O2	-0.3	Terpenoid	KEGG	-1.1	-2.4	-1.3
1	AA_11	1.74	[M+H]+	104.107407	Choline	C5H14NO	4.1	Choline	metlin	1.1	-6625.2	-1.2
1	AA_01	2.12	[M+H]+	177.061813	Allantoic acid	C4H8N4O4	-0.1	Alpha amino acid	magma	1.1	-2.2	1.4
1	AA_07	3.12	[M+H]+	206.102081	N-Acetyl-D-fucosamine	C8H15NO5	-0.9	Amino sugar	magma	1.0	-373.0	1.4
1	AA_57	2.51	[M+H]+	98.984627	Phosphoric acid	H3O4P	4.6	non-metal phosphate	HMDB	1.1	-11.3	1.2
1	AA_29	44.85	[M-H]-	271.061066	4',5,8-Trihydroxyflavanone	C15H12O5	-0.9	Flavonoid	HMDB	-1.2	-2.3	-1.3
1	AA_30	38.32	[M-H]-	287.05603	3',5,5',8-Tetrahydroxyflavanone; (S)-form	C15H12O6	-0.3	Flavonoid	Dictionary of natural compound	-1.1	-2.6	-1.6
1	AA_79	41.18	[M+H]+	235.169098	Dihydrodeoxyarteannuin B	C15H22O2	-0.7	Terpenoid	Knapsack	-1.2	-2.0	-1.3
1	AA_34	29.35	[M+H]+	641.171082	Patuletin 3-O-rutinoside	C28H32O17	-0.2	Flavonoid	Knapsack	-1.1	-2.5	-1.3
1	AA_34_2	29.34	[M-H]-	639.15625	Patuletin 3-O-rutinoside	C28H32O17	-0.7	Flavonoid	Knapsack	-1.0	-2.5	-1.3
1	AA_31	43.45	[M+H]+	347.076202	5,6,3',4'-Tetrahydroxy-3,7-dimethoxyflavone	C17H14O8	0.2	Flavonoid	Knapsack	-1.1	-2.5	-1.3
1	AA_76	41.87	[M+H]+	235.169098	Artemisinic acid	C15H22O2	-0.7	Terpenoid	magma	-1.3	-4.4	-1.7
1	AA_90	34.22	[M-H]-	507.114197	11-O-Syringylbergenin	C23H24O13	-1.0	Benzoic acid	Pubchem	1.1	-2.4	1.1
1	AA_62	40.98	[M-H]-	517.134705	Medicarpin 3-O-glucoside-6'-malonate	C25H26O12	-0.9	Pterocarpan	magma	-1.0	-2.3	-1.2
1	AA_81	22.00	[M+H]+	105.070274	Styrene	C8H8	3.8	Styrene	magma	1.2	-10.5	-1.0
1	AA_15	16.88	[M-H]-	243.134827	Leucyl-Hydroxyproline	C11H20N2O4	-0.8	Dipeptide	HMDB	-1.3	-25.0	-1.7
1	AA_49	47.25	[M-H]-	551.213013	Prupaside	C27H36O12	-0.7	Lignan glycoside	HMDB	-1.1	-2.0	-1.1
1	AA_84	29.21	[M-H]-	347.170929	Foeniculoside V	C16H28O8	-0.6	Terpene glycoside	HMDB	-1.0	-3.6	-1.1
1	AA_10	6.94	[M-H]-	138.055939	Gabaculine	C7H9NO2	-0.6	Benzoic acid	KEGG	-1.1	-13.0	-1.5
1	AA_27	32.91	[M-H]-	415.197205	Ethyl 7-epi-12-hydroxyjasmonate glucoside	C20H32O9	-0.4	Fatty acyl glycosides of mono- and disaccharides	Metlin	1.0	-3.3	-1.2
1	AA_85	23.11	[M-H]-	347.170959	Nepetariaside	C16H28O8	-0.5	Terpene glycoside	HMDB	1.0	-3.1	-1.2
1	AA_38	32.21	[M-H]-	243.123566	4-Oxododecanedioic acid	C12H20O5	-0.9	Hydroxy fatty acid	Metlin	-1.1	-4.4	-1.2
1	AA_16	13.28	[M+H]+	245.149445	Isoleucyl-Hydroxyproline	C11H20N2O4	-0.6	Dipeptide	HMDB	-1.1	-8.6	-1.3
1	AA_17	5.81	[M+H]+	231.133804	Valyl-Hydroxyproline	C10H18N2O4	-0.6	Dipeptide	HMDB	-1.1	-10.0	-1.4
1	AA_91	26.11	[M+H]+	227.127609	1-Acetoxy-7-hydroxy-3,7-dimethyl-2E,5E-octadien-4-one	C12H18O4	-0.8		Knapsack	-1.1	-5.4	-1.5
1	AA_87	28.32	[M+H]+	175.148239	1,2,3,4-Tetrahydro-1,4,6-trimethyl-naphthalene	C13H18	-0.2	Tetralin	HMDB	-1.0	-3.4	-1.3
1	AA_22	42.91	[M-H]-	469.22879	3-Hydroxy-6-methylheptyl 2-O-?-D-glucopyranosyl-?-D-glucopyranoside	C20H38O12	-0.5	Fatty acyl glycosides of mono- and disaccharide	Metlin	-1.1	-13.1	-1.9
1	AA_71	24.93	[M-H]-	311.113586	p-Coumaryl alcohol 4-O-glucoside	C15H20O7	-0.4	monolignol_cinnamyl alcohol beta-D-glucosid	magma	1.1	-3.3	-1.3

Table S6. (Continued)

Cluster Number	Metabolite ID	RT (m)	m/z	Mass(D)	Compound	Formula	Δ ppm to DB	Classification	data base	Fold change		
										MB	*Pbg*	*Pf* SS101
1	AA_21	51.43	[M-H]-	333.191803	3,7-Dimethyl-5-octene-1,7-diol 1-glucoside	C10H20O2	-0.2	Fatty acyl glycosides of mono- and disaccharide	HMDB	1.0	-6.4	-1.7
1	AA_59	22.32	[M-H]-	297.097839	Picein	C14H18O7	-0.5	Phenolic glycosides	KNAPSACK	1.1	-6.5	-1.4
1	AA_50	41.38	[M-H]-	187.097504	Azelaic acid or (C17878)	C9H16O4	-0.4	Medium-chain fatty acid	magma	1.1	-4.5	-1.4
1	AA_48	19.59	[M-H]-	172.097855	N-Acetyl-L-leucine or (C10173)	C8H15NO3	-0.4	Leucine and derivative	magma	-1.0	-3.4	1.0
1	AA_72	21.99	[M-H]-	461.166443	Verbasoside or (HMDB39233)	C20H30O12	0.0	Monolignol	HMDB	1.1	-6.9	-1.1
1	AA_02	6.39	[M-H]-	315.10849	Hydroxytyrosol 1-O-glucoside	C14H20O8	-0.2	o-glycosyl compound	HMDB	1.0	-2.3	-1.0
1	AA_25	19.29	[M+H]+	403.196198	D-Linalool 3-(6''-malonylglucoside) or (HMDB0031763)	C19H30O9	-0.2	Fatty acyl glycoside	HMDB	-1.0	-2.0	-1.1
1	AA_36	2.33	[M+H]+	261.037048	Glucose 6-phosphate	C6H13O9P	0.2	Hexose phosphate	HMDB	-1.0	-4.7	-1.1
2	AA_56	53.51	[M+H]+	137.132401	beta-Pinene	C10H16	-0.6	Monoterpen	magma	1.8	2.6	1.3
2	AA_74	54.32	[M+H]+	233.153412	Isoalloalantolactone (Helenin)	C15H20O2	-0.7	Terpenoid	KEGG	-796.2	2.2	-2.3
2	AA_73	12.94	[M-H]-	353.087616	Scopolin or (C00852)	C16H18O9	-0.3	Hydroxycinnamate	magma	-1.4	3.5	-1.0
2	AA_05	3.75	[M+H]+	118.086517	Valine	C5H11NO2	2.2	Amino acid	HMDB	-1.0	90.3	1.1
2	AA_08	42.95	[M+H]+	135.116821	p-Cymene	C10H14	0.0	Terpenoids	HMDB	1.4	2.6	1.3
2	AA_63	33.27	[M-H]-	515.119141	1,3-Dicaffeoylquinic acid I	C25H24O12	-0.7	Hydroxycinnamate	Metlin	1.3	3.2	-1.1
2	AA_54	30.97	[M-H]-	417.176422	2-[4-(3-Hydroxypropyl)-2-methoxyphenoxy]-1,3-propanediol 1-glucoside	C19H30O10	-0.5	Hydroxycinnamate	HMDB,DNP	1.3	6.1	2.1
2	AA_18	51.66	[M+H]+	179.085541	2,12-Tetradecadiene-4,6,8,1-tetrayne	C14H10	0.1	Enyme	HMDB	2.6	14.5	5.4
2	AA_61	5.78	[M+H]+	167.070328	3-Hydroxyhydrocinnamic acid	C9H10O3	0.4	Phenylpropanoic acid	ChemSpider	24.4	179.8	51.7
2	AA_64_2	29.92	[M-H]-	515.119141	1,3-Dicaffeoylquinic acid II	C25H24O12	-0.7	Hydroxycinnamate	HMDB	1.3	5.5	1.3
2	AA_55	33.39	[M-H]-	371.134491	Syringin	C17H24O9	-0.6	Hydroxycinnamate	Knapsack	-1.0	2.0	1.1
2	AA_88	4.05	[M-H]-	173.009048	Aconitic acid	C6H6O6	-0.7	Tricarboxylic acid	Metline	-1.0	4.7	-1.1
2	AA_86	49.47	[M-H]-	403.197113	Pisumionoside	C19H32O9	-0.6	Terpene glycoside	HMDB	1.0	4.6	1.2
2	AA_44	5.09	[M+H]+	265.154816	Feruloylputrescine	C14H20N2O3	0.6	Hydroxycinnamate	magma	-1.1	5.9	1.3
2	AA_77	50.95	[M+H]+	221.189926	Artemisinic alcohol	C15H24O	-0.3	Sesquiterpenoid	magma	1.1	2.5	1.0
2	AA_75	46.14	[M-H]-	285.170746	1,2,6,7-Tetraoxaspiro[7.11]nonadecan-3-one	C15H26O5	0.0	Sesquiterpenoid	Chemspider	1.2	3.7	1.4
2	AA_39	32.43	[M-H]-	193.0504	Methyl caffeate	C10H10O4	-1.2	Hydroxycinnamate	KEGG	1.0	4.7	-1.2
2	AA_78	45.50	[M-H]-	283.154999	Dihydroartemisinin or Arteannuin H	C15H24O5	-0.3	Sesquiterpenoid	metlin_HMDB	-1.2	2.9	-1.1
2	AA_20	13.34	[M-H]-	393.176544	cis-3-Hexenyl b-primeveroside	C17H30O10	-0.2	Fatty acyl glycoside	HMDB	1.0	2.3	1.0
2	AA_83	5.79	[M-H]-	391.124542	Shanzhiside	C16H24O11	-0.1	Terpene glycoside	ChemSpider	1.1	6.7	1.9
2	AA_45	15.65	[M-H]-	419.155731	Lamioside	C18H28O11	-0.5	Iridoid	KEGG	1.0	3.1	1.2
2	AA_24	46.98	[M+H]+	401.180481	Corchoionoside B	C19H28O9	-0.3	Fatty acyl glycoside	HMDB	-1.1	3.7	-1.1
2	AA_13	29.86	[M+H]+	163.038605	7-Hydroxycoumarin	C9H6O3	-2.2	Coumarin	Knapsack	-1.1	69.2	-1.1
2	AA_26	40.84	[M-H]-	501.233978	Eriojaposide A	C24H38O11	-0.3	Fatty acyl glycoside	HMDB	1.0	5.1	1.3

Table S6. (Continued)

Cluster Number	Metabolite ID	RT (m)	m/z	Mass(D)	Compound	Formula	Δ ppm to DB	Classification	data base	Fold change		
										MB	*Pbg*	*Pf* SS101
2	AA_14	16.21	[M-H]-	129.055664	Mevalonolactone	C6H10O3	-0.4	Delta valerolactone	HMDB	-1.2	2.2	-1.2
2	AA_37	9.38	[M-H]-	175.061066	3-Propylmalate	C7H12O5	-0.9	Hydroxy fatty acid	magma	-1.1	5.9	1.6
2	AA_04	1.97	[M-H]-	132.030121	Aspartic acid	C4H7NO4	-0.8	Amino acid	HMDB	1.1	3.8	1.2
2	AA_42	13.68	[M-H]-	341.087555	Caffeic acid 3-glucoside	C15H18O9	-0.5	Hydroxycinnamate	magma	1.2	4.7	1.3
2	AA_35	27.63	[M-H]-	447.092834	Luteolin 7-glucoside	C21H20O11	-1.0	Flavonoid	HMDB	-1.1	2.3	-1.2
2	AA_66	36.03	[M-H]-	529.134766	1-Feruloyl-5-caffeoylquinic acid	C26H26O12	-0.7	Hydroxycinnamate	Metlin, HMDB	1.1	170.1	5.6
2	AA_64	41.77	[M-H]-	543.150513	1,5-Diferuloylquinic acid	C27H28O12	-0.5	Hydroxycinnamate	HMDB	-1.7	29.4	-1.7
2	AA_68	24.36	[M+H]+	369.118042	5-O-Feruloylquinic acid	C17H20O9	0.2	Hydroxycinnamate	Metlin	-1.2	5.8	-1.0
2	AA_40	21.96	[M-H]-	367.10321	O-Feruloylquinate	C17H20O9	-0.6	Hydroxycinnamate	KEGG	-1.3	13.5	-1.1
2	AA_40_2	21.96	[M+H]+	369.118011	O-Feruloylquinate	C17H20O9	0.1	Hydroxycinnamate	KEGG	-1.3	13.5	-1.1
2	AA_47	26.19	[M-H]-	389.108795	Monotropein	C16H22O11	-0.4	Iridoid o-glycoside	magma	1.0	13.8	1.0
2	AA_09	17.77	[M-H]-	308.077576	N-Feruloylaspartic acid	C14H15NO7	0.0	Aspartic acid	HMDB	1.1	49.6	1.0
2	AA_58	2.41	[M-H]-	133.01416	Malic acid	C4H6O5	-0.7	Organic acid	MSMS	-1.4	6.7	-1.4
2	AA_65	36.37	[M-H]-	529.134766	1-Caffeoyl-5-feruloylquinic acid	C26H26O12	-0.7	Hydroxycinnamate	HMDB, PubChem	-1.1	10.8	1.1
2	AA_69	14.88	[M+H]+	355.102203	Chlorogenic Acid	C16H18O9	-0.4	Hydroxycinnamate	Metlin	-1.1	2.6	-1.1
2	AA_67	36.03	[M+H]+	531.149231	4-O-Caffeoyl-3-O-feruloylquinic acid	C26H26O12	-0.9	Hydroxycinnamate	HMDB	-19.4	13.3	-1.6
2	AA_46	15.65	[M+H]+	213.112045	7-Deoxyloganetin	C11H16O4	-0.6	Terpenoid	KEGG	-1.0	2.7	1.1
2	AA_89	2.99	[M-H]-	191.019699	Citric acid	C6H8O7	-0.1	Tricarboxylic acid	HMDB	1.0	9.5	-1.5
2	AA_12	33.63	[M+H]+	357.118011	1-Feruloyl-D-glucose	C16H20O9	0.1	Coumaric acid	KEGG	-1.3	9.5	-1.1
2	AA_52	3.54	[M-H]-	159.029785	Oxoadipic acid	C6H8O5	-0.9	Medium-chain keto acids and derivatives, Carboylic acid	KEGG	2.2	60.3	2.2
2	AA_82	3.68	[M-H]-	191.019745	2,5-Diketogulonic acid	C6H8O7	0.1	Sugar acid	HMDB	1.3	9.4	-1.2
2	AA_70	33.14	[M+H]+	339.1073	p-Coumaroyl quinic acid	C16H18O8	-0.4	Hydroxycinnamate	magma	-1.3	22.5	-1.1
2	AA_41	33.15	[M+H]+	357.118011	1-O-Feruloyl-beta-D-glucose	C16H20O9	0.0	Hydroxycinnamate	ChemSpider	-1.3	21.8	-1.1
2	AA_51	18.07	[M-H]-	131.071274	6-Hydroxyhexanoate	C6H12O3	-0.7	Medium-chain hydroxy acid	HMDB	1.1	6.6	-1.4
2	AA_43	26.72	[M+H]+	165.054703	p-Coumaric acid	C9H8O3	0.5	Hydroxycinnamate	HMDB	1.2	6.2	1.0
3	AA_28	42.78	[M+H]+	129.127426	octanal/1-Octen-3-ol (C14272)	C8H16O	0.4	Fatty alcohol	Metlin, KNApSAck	-1.2	9.3	11.0
3	AA_19	26.99	[M-H]-	503.249634	Blumenol C O-[apiosyl-(1->6)-glucoside], (3S,7E,9R)-4,7-Megastigmadiene-3,9-diol 9-[apiosyl-(1->6)-glucoside]	C24H40O11	-0.4	Fatty acyl glycoside	Metlin	1.2	6.3	8.7
3	AA_60	31.57	[M+H]+	331.138672	(±)-3-(4-Hydroxyphenyl)-1,2-propanediol 4'-O-glucoside	C15H22O8	-0.3	Phenylpropanod	Metlin	1.2	2.1	2.4
3	AA_06	2.97	[M-H]-	128.035217	Pyroglutamic acid, Pyrroline hydroxycarboxylic acid, 4-Oxoproline	C5H7NO3	-0.8	Amino acid	Metlin	-1.1	1.2	2.1
3	AA_03_2	1.70	[M-H]-	173.104233	Arginine	C6H14N4O2	-1.0	Amino acid	Metlin, HMDB	1.1	-2.3	2.4
3	AA_03	1.59	[M+H]+	175.118973	Arginine	C6H14N4O2	0.1	Amino acid	Metlin, HMDB	1.2	-1.6	2.5

Table S7. Fold changes of metabolites in shoots of Arabidopsis (Arab), Broccoli (Bro) and Artemisia (Art) upon treatment of the roots with different rhizobacterial genera. The metabolites listed here have been associated with human health. *Pf* SS101: *Pseudomonas fluorescens* SS101, MB: *Microbacterium* sp., *Pbg*: *Paraburkholderia graminis*.

Plant	Compound	Compound classification	Fold changes			Health treat	Reference
			MB	Pbg	*Pf* SS101		
Arab	Glucoerucin	Aliphatic GLS	-1.43	-1.71	-1.18	Fungicidal (soil born pathogen) activity of enzyme derivered production of glucoiberin, Cancer prevention: inhibition of cell demage indeced by H2O2 in hepa1c1c7 cell line by myrosinase treated this glucosinlate, oomycete, antioxidative, cancer chemopreventive	(Manici *et al*., 1999; Manici *et al*., 2000; Zhu & Loft, 2003; Barillari *et al*., 2005; Razis *et al*., 2011)
Arab	Glucohirsutin	Aliphatic GLS	3.07	-5.71	4.48	Resistance to insect hervivory	(Beekwilder *et al*., 2008)
Arab	Glucoraphanin	Aliphatic GLS	1.39	-25.11	1.19	Cancer prevention: inhibition of cell demage indeced by H2O2 in hepa1c1c7 cell line by myrosinase treated this glucosinlate, Anticarcinogen sulforaphane (catalized by myrosinase)	(Matusheski & Jeffery, 2001; Zhu & Loft, 2003)
Arab	Camalexin	Alkaloid	12.8	64.2	20.5	Antiproliferative activity against a human breast cancer cell line	(Glawischnig, 2007)
Arab	Indole-3-acetic acid	Alkaloid	14.4	39.9	8.4	Plant growth regulator	(Spaepen *et al*., 2007)
Arab	Cyanidin delivatives	Anthocyanin	2.2	45.3	1.4	Antioxidants, which help to prevent neuronal diseases, cardiovascular illnesses, cancer, diabetes, inflammation, and many such others diseases	(Yousuf *et al*., 2016)
Arab	Gabaculine	Benzoic acid	-1.94	-54.55	-2.32	GABA transaminase inhibitor	(Rando & Bangerter, 1977)
Arab	Phenylacetic acid	Carboxylic acid ester	4.25	46.04	2.21	Natural auxin	(Wightman & Lighty, 1982)
Arab	Trimethoxycinnamic acid	Coumaric acid	6.7	100.3	1.4	Antidepressant-like effects on mice in forced swimming test and anti-stress effects on rat	(Nakazawa *et al*., 2003; Kawashima *et al*., 2004)
Arab	Ayapin	Coumarin	5.2	10.7	1.4	Antifungal activity	(Urdangarin *et al*., 1999)
Arab	Fraxetin	Coumarin	5.32	11.39	1.36	Neuroprotective effect, antioxidative, Antihyperglycemic effect, Antitumor and antimetastatic actions	(Martín-Aragón *et al*., 1997; Molina-Jiménez *et al*., 2004; Murali *et al*., 2013; Kimura & Sumiyoshi, 2015)
Arab	Fraxin	Coumarin	2.06	8.45	1.37	Antioxidative	(Whang *et al*., 2005)
Arab	Scoparone	Coumarin	-1.0	-23.6	1.4	Antioomycete, prevention and therapy of liver injury	(Afek & Sztejnberg, 1988; Zhang *et al*., 2013)
Arab	Hesperidin	Flavonoid	-1.21	22.99	-1.05	Anti-inflammatory	(Guardia *et al*., 2001)
Arab	Isorhamnetin glycosides	Flavonoid	2.28	3.93	1.54	free radical scavenging, cancer cell apoptosis induction	(Hyun *et al*., 2006; Antunes-Ricardo *et al*., 2014)
Arab	Kaempferitrin	Flavonoid	2.3	6.2	1.5	inhibits insulin stimulated GLUT4 translocation and glucose uptake in 3T3-L1 adipocytes	(Prasad *et al*., 2009)
Arab	Rutin	Flavonoid	2.23	21.22	-1.03	Antioxidative, Anti-inflammatory, cancer chemopreventive	(Deschner *et al*., 1991; Guardia *et al*., 2001; Yang *et al*., 2008)
Arab	Sinapic acid	Hydroxycinnamate	1.5	6.0	-1.3	Anti-Inflammatory Effects, Anxiolytic-like effects, Cerebral protective and cognition-improving effects	(Karakida *et al*., 2007; Yoon *et al*., 2007; Yun *et al*., 2008)
Arab	Geniposide	Iridoid	8.01	30.89	2.14	Anti-inflammatory, Antithrombotic, hypoglycemic effect	(Suzuki *et al*., 2001; Koo *et al*., 2006; Wu *et al*., 2009)
Arab	Fumaric acid	Organic acid	4.69	1.57	1.80	Treatment for Psoriasis vulgaris and decrease of multifocal leukoencephalopathy (PML)	(Ermis *et al*., 2013)
Arab	Salicylic Acid	Organic acid	6.22	40.65	1.37	Provoke SAR	(Delaney *et al*., 1994)

Table S7. (Continued)

Plant	Compound	Compound classification	Fold changes			Health treat	Reference
			MB	Pbg	*Pf* SS101		
Bro	Glucoraphanin	Aliphatic GLS	-1.06	-2.05	1.11	Cancer prevention: inhibition of cell demage indeced by H2O2 in hepa1c1c7 cell line by myrosinase treated this glucosinlate, Anticarcinogen sulforaphane (catalized by myrosinase)	(Matusheski & Jeffery, 2001; Zhu & Loft, 2003)
Bro	Ascorbic acid	Butenolide	2.01	3.73	4.53	Antioxidative, Anticancer activities	(Fraga *et al*., 1991; Arrigoni & De Tullio, 2002; Chen *et al*., 2005)
Bro	Dehydroascorbic acid	Butenolide	1.47	2.73	3.38	Cerebroprotection	(Huang *et al*., 2001)
Bro	Scopoletin	Coumarin	1.49	3.91	-8.88	Inhibited PC3 proliferation by inducing apoptosis of PC3 cells (human prostate cancer cell line), antithyroid, antioxidative and antihyperglycemic activity	(Liu *et al*., 2001; Panda & Kar, 2006)
Bro	beta-Damascenone	Enones	1.09	1.42	2.64	Antispasmodic activity	(Pongprayoon *et al*., 1992)
Bro	Kaempferol glycosides	Flavonoid	-1.00	1.25	2.40	Neuroinflammation, anti-obesity and anti-diabetic effects, inflammation, allelopathic role	(Fang *et al*., 2005; Fiorentino *et al*., 2009; Zhu *et al*., 2011; Yu *et al*., 2013; Zang *et al*., 2015)
Bro	Rutin	Flavonoid	1.16	1.91	3.36	Antioxidative, Anti-inflammatory, cancer chemopreventive activities	(Deschner *et al*., 1991; Guardia *et al*., 2001; Yang *et al*., 2008)
Bro	Caffeic acid	Hydroxycinnamate	1.39	2.52	3.23	Antimitogenic, anticarcinogenic, antiinflammatory, and immunomodulatory properties, antioxidative activities	(Huang *et al*., 1988; Natarajan *et al*., 1996; Gülçin, 2006)
Bro	Ferulic acid	Hydroxycinnamate	1.30	1.90	3.15	Cancer chemopreventive effect	(Huang *et al*., 1988)
Bro	Sinapic acid	Hydroxycinnamate	1.08	1.51	2.02	Anti-Inflammatory, Anxiolytic-like, Cerebral protective and cognition-improving effects	(Karakida *et al*., 2007; Yoon *et al*., 2007; Yun *et al*., 2008)
Bro	4-Methoxyglucobrassicin	Indolic GLS	-1.02	1.01	2.30	Antioxidative effect	(Kim & Ishii, 2006)
Bro	Glucobrassicin	Indolic GLS	1.51	3.96	5.09	Cancer chemopreventive effect	(Park *et al*., 2013)
Bro	Neoglucobrassicin	Indolic GLS	-1.15	1.15	3.51	Breakdown products induce cancer chemopreventinve activity	(Haack *et al*., 2010)
Bro	Gentiopicroside	Iridoid	1.37	2.01	3.54	Hepatoprotective effect	(Kondo *et al*., 1994)
Bro	Ascorbigen	Isosorbide	2.24	6.44	7.05	Degraded product has anticarcinogenic effect, induction of phase I and II enzyme involved in the detoxification of xenobiotics	(Wagner & Rimbach, 2009)
Bro	Chlorogenic acid	Quinic acid	1.29	2.60	3.88	Cancer chemopreventive, antioxidative activities	(Huang *et al*., 1988; Sato *et al*., 2011)
Art	Gabaculine	Benzoic acid	-1.13	-13.04	-1.48	GABA transaminase inhibitor	(Rando & Bangerter, 1977)
Art	7-Hydroxycoumarin	Coumarin	-1.06	69.18	-1.08	Anti-tumour activity	(Lopez-Gonzalez *et al*., 2004)
Art	Octanal	Fatty alcohol	-1.16	9.30	10.95	Antifungal activity	(Zhou *et al*., 2014)
Art	Luteolin 7-glucoside	Flavonoid	-1.08	2.28	-1.25	Anti-inflammatory activity	(Hu & Kitts, 2004)
Art	Puerarin xyloside	Flavonoid	1.22	13.05	2.36	Anti-osteoporotic , Antitumour activities	(Chen *et al*., 2016; Li *et al*., 2016; Zhang *et al*., 2018)
Art	Caffeic acid 3-glucoside	Hydroxycinnamate	1.18	4.73	1.26	Anti-inflammatory activity, increases osteoblastic bone formation and prevents bone loss in ovariectomized mice	(Wang *et al*., 2014; Zhang *et al*., 2016)
Art	p-Coumaric acid	Hydroxycinnamate	1.19	6.16	1.03	Protects rats hearts against doxorubicin-induced oxidative stress in the heart and H82 Antioxidative, Antibacterial activities	(Zang *et al*., 2000; Abdel-Wahab *et al*., 2003; Lou *et al*., 2012)
Art	Methyl caffeate	Hydroxycinnamate	1.03	4.67	-1.17	Antimicrobial and Antimycobacterial Activities	(Balachandran *et al*., 2012)
Art	Azelaic acid	Medium-chain fatty acid	1.08	-4.46	-1.36	Treatment on melasma	(Baliña & Graupe, 1991)
Art	Syringin	Phenolic glycoside	-1.04	2.05	1.11	Anti-inflammatory, antinociceptive and hypoglycemic effect, Antifeedant property, and anti-allergic effect	(Cho *et al*., 2001; Choi *et al*., 2004; Cis *et al*., 2006; Niu *et al*., 2008)
Art	Chlorogenic acid	Quinic acid	-1.08	2.61	-1.11	Cancer chemopreventive, antioxidative activities	(Huang *et al*., 1988; Sato *et al*., 2011)

Table S7. (Continued)

Plant	Compound	Compound classification	Fold changes			Health treat	Reference
			MB	Pbg	*Pf* SS101		
Art	Artemisinic alcohol	Sesquiterpenoid	1.09	2.48	1.03	Precousor of Artemisinin	
Art	Artemisinin	Sesquiterpenoid	-1.10	1.09	-1.14	Antimalarial and Anticancer activities, inhibitors of hepatitis B virus	(Singh & Lai, 2004; Romero *et al.*, 2005; Dondorp *et al.*, 2009)
Art	Dihydroartemisinin	Sesquiterpenoid	-1.25	2.95	-1.10	Antimalarial activity, induction of cytotoxicity on Human breast cancer cells, induction of apaotosis on ovarian cancer cells, inhibition of angiogenesis, pancreatic cancer cells	(Singh & Lai, 2001; Chen *et al.*, 2004; Chen, H *et al.*, 2009; Chen, T *et al.*, 2009)